Feed forward control of estimated wind speed

E.L. van der Hooft; T.G. van Engelen

December 2003

Acknowledgment
This report is issued in the framework of the DEN program, supported by Novem, a department of the Dutch Ministry of Economic Affairs. I like to thank Pieter Schaak for his supporting activities to this report, comments and project management.

Eric van der Hooft,
Petten, December 31st, 2003

Keywords:
Wind turbine control, Pitch Control, Power Control, Optimisation, Variable speed control

Abstract

A control structure ‘feed forward of estimated wind speed’ is described, as it were: ‘the wind turbine rotor will be used as a wind meter’.

The control structure is based on ‘estimation’ of wind speed as well as a non-linear compensation of a wind speed dependent pitch speed setpoint, which is optimised to maintain (stationary) rated electric power. It is required to know the rotor properties with moderate accuracy.

In time domain simulations, inclusion of a feed forward of estimated wind speed control action has shown to be a powerful extension to current ECN wind turbine control structures:

- reduction of rotor speed variations: $\sim$ 0.2 rpm decreased standard deviation;
- improved turbine response to large wind gusts;
- increase of energy yield of $\sim$ 0.9%;

For reasons of simplicity and robustness, a tabular implementation approach is preferred above polynomial implementation. The resulting brief algorithm uses small sized tables, requires low hardware requirements and needs a minimum of easy interpretable parameters for design and tuning.

Both stability, robustness and parametric uncertainties were observed. The addition control loop has a slightly positive effect on overall stability and robustness. Appeared offsets in the estimated wind speed value due to parameter uncertainties do not have impact on the effectuation of the wind speed feed forward loop.

CONTENTS

1 INTRODUCTION

Wind turbine power control algorithms for variable speed / active pitch turbines at above rated wind speed conditions, are often based on rotor speed regulation by pitch actuation and power production by generator torque control. Rotor speed regulation is then achieved by feed back of rotor speed and rotor acceleration to the pitch speed (PD-control), or similar, to the pitch angle (PI-control).

The control performance of using the rotor speed / acceleration as feedback quantity is mainly restricted by the huge rotor inertia. Rotor speed fluctuations are obvioulsy a consequence of their cause: disturbing wind fluctuation or gusts. Direct feed forward of measured wind speed (fluctuations) will be impossible, because wind speed can only be measured in one specific point and location, while the 'rotor effective wind speed' is required.

In this report the approach of 'feed forward of estimated wind speed' is described in detail. Popularly, the wind turbine rotor will be used as a wind meter. The control structure aimes to improve the power control performance and is based on 'estimation' of wind speed by using the energy balance:

'the sum of electric energy (production), rotational energy (inertia) and energy losses (heat) equals to the aerodynamic energy as captured by the turbine rotor',

as well as a non-linear compensation of a wind speed dependent pitch speed setpoint, which is optimised to maintain (stationary) rated electric power. Furthermore, it is assumed that rotor properties are a priori known with moderate accuracy.

The first chapter of this report will describe the relevant (dynamic) turbine behaviour, which will be basic for design of the proposed control structure.

Because the feed forward will be an optimisation extension to the current ECN control structure (pitch control, electric torque control), the basic power control algorithm is described in general terms in chapter 3.

Chapter 4 will describe in detail the principles wind speed estimation and effectuation to a feed forward mechanism in detail (section 4.1). Two implementation approaches are discussed: polynomial implementation (section 4.3) and tabular implementation (section 4.4).

In chapter 5 the performance of the proposed control structure is determined by comparison of time domain simulation results with and without the feed forward, stability analysis and parametric uncertainty behaviour.

Finally, conclusions are made and shortly listed in chapter 6.

2 WIND TURBINE BEHAVIOUR

In this chapter relevant dynamic behaviour of a typical variable speed, active pitch to vane wind turbine is explained shortly: aerodynamic conversion, rotational mechanics and electric conversion. Furthermore, the model of wind speed as experienced by the turbine rotor is clarified.

2.1 Aerodynamic conversion

The aerodynamic conversion proces of the turbine rotor is approximated with quasi stationary non-linear equations for aerodynamic torque, $T_{\rm a}$, and aerodynamic power, $P_{\rm a}$:

$$T_{\rm a} = C_{\rm q}(\lambda,\theta)\cdot\tfrac{1}{2}\rho_{\rm air}\pi R_{\rm b}^3\cdot(V_{\rm w}-\dot{x}_{\rm nd})^2 \quad (2.1)$$

$$P_{\rm a} = C_{\rm p}(\lambda,\theta)\cdot\tfrac{1}{2}\rho_{\rm air}\pi R_{\rm b}^2\cdot(V_{\rm w}-\dot{x}_{\rm nd})^3 \quad (2.2)$$

with the tip to wind speed ratio, λ :

$$\lambda = \frac{\Omega_{\rm r}\cdot R_{\rm b}}{(V_{\rm w}-\dot{x}_{\rm nd})} \quad (2.3)$$

In eq.(2.1) the reference of the tower top displacement speed, $\dot{x}_{\rm nd}$, is (opposite) related to the mean wind speed, $\overline{V}_{\rm w}$ in longitudinal sense.
The torque coefficient $C_{\rm q}$ can be determined from the power coefficient $C_{\rm p}$ by

$$C_{\rm q}(\lambda,\theta) = C_{\rm p}(\lambda,\theta)/\lambda. \quad (2.4)$$

Both $C_{\rm p}$ and $C_{\rm q}$ are dependent of the tip to wind speed ratio λ and the pitch angle θ . For the a typical rotor, the power and thrust coefficient characteristics are shown in fig.(2.1). The curves in fig.(2.1) are normalised to their maximum values; usually, the maximum $C_{\rm q}$ value will be around 0.065, while the maximum $C_{\rm p}$ value will be around 0.48. The curves, will be used as 'aerodynamic a priori knowledge' for wind speed estimation and feed forward control. Because they are not a function 'in mathematical sense', the typical shape will give inevitable restrictions (chapter 4).

For control purposes, the dynamic effects of the wake (dynamic inflow) can not easily be neglected, specifically not for the low wind speed region. Though, in [2] it has been shown that a simple (scheduled) linear compensating structure, has appeared to be effective in dealing with this phenomenon. Therefore, dynamic inflow effects will be further ignored (ideal compensation).

2.2 Rotating mechanical system

The turbine rotor will accelerate or decelerate if there's a difference between aerodynamic torque, $T_{\rm a}$ and electric torque, $T_{\rm e}$. If a stiff coupling is assumed between rotor and generator, then $\Omega_{\rm r}$ = $\Omega_{\rm g}$ and the mechanical equation of the drive system can be simply expressed by (eq.(2.5))

$$J_{\rm t}\cdot\dot{\Omega}_{\rm r} = T_{\rm a} - T_{\rm l} - T_{\rm e} \quad (2.5)$$

in which $J_{\rm t}$ is defined as total 'slow speed shaft equivalent' inertia:

$$J_{\rm t} = J_{\rm r} + i_{\rm gb}^2\cdot J_{\rm g}; \quad (2.6)$$

Aerodynamic losses are divided in a constant part ('Coulomb friction') and a speed dependent part ('rotation losses'):

$$T_{\rm l} = C_{\rm c} + C_{\Omega_{\rm r}}\cdot\Omega_{\rm r} \quad (2.7)$$

A simple approximation can be found by neglection of 'constant losses' and determination of the rotation losses from the overall efficiency at rated conditions.

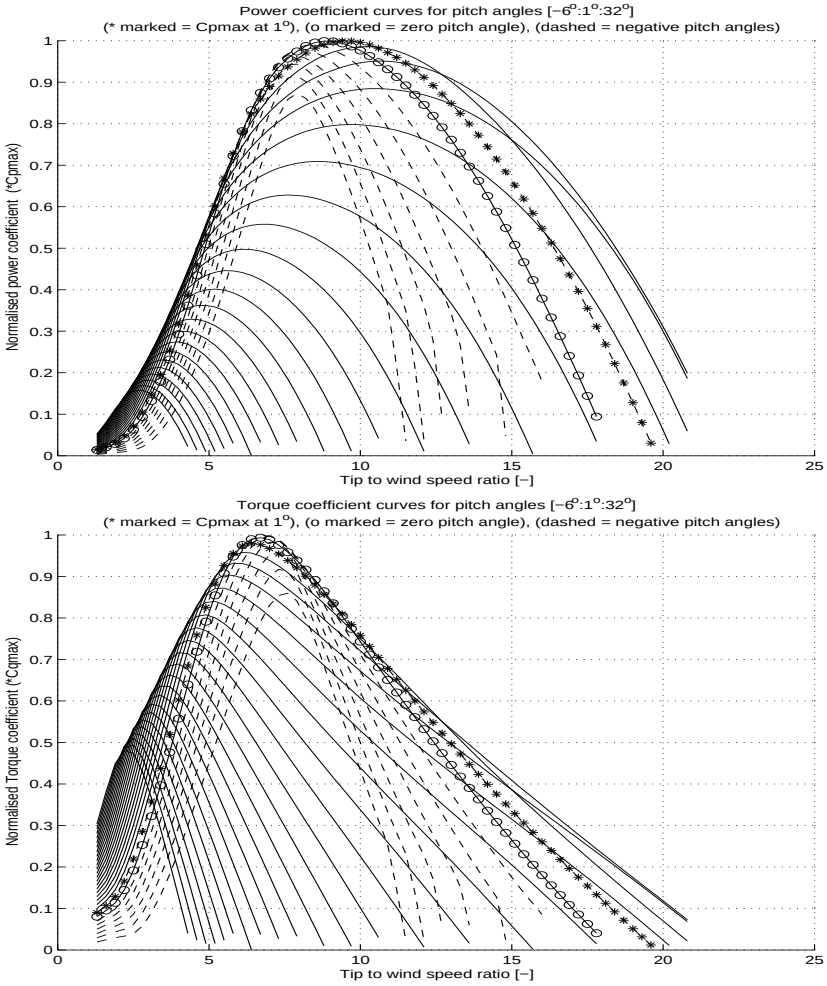

Figure 2.1: *Power- en torque coefficient curves of a typical turbine*

This simple drive train model is only valid if drive train or collective lead-lag vibrations (if coupled to the blades) are:

- neglectable from nature (stiff shaft), or
- reduced sufficienty by active damping [3] or
- filtered out from (measured) feedback signals.

2.3 Electric conversion

During full load operation (above rated wind speed) the power production of the generator will be determined by the stationary relationship between rotor speed and electric torque. Basically, this implies constant rated power production, $P_{\mathrm{e}}^{\mathrm{rat}}$:

$$T_{\mathrm{e\ ,full}}^{*} = \frac{P_{\mathrm{e}}^{\mathrm{rat}}}{\tilde{\Omega}_{\mathrm{r}}^{\mathrm{f}}} \tag{2.8}$$

Sideward tower movements ('naying') will have influence on evolving electric torque due to rotor speed variations. Additional (dynamic) torque setpoint components $T_{\mathrm{e,ctrl}}^{*}$ can be added

to achieve improved turbine control [3].

$$T_{\rm e}^* = T_{\rm e}^*(\Omega_{\rm r} - \frac{\dot{x}_{\rm ny}}{Z_{\rm t}}) + T_{\rm e,ctrl}^* \tag{2.9}$$

On the condition that:

- high speed switching power electronics are able to set electric generator torque almost instantaneously with respect to the mechanical dynamics;
- (high frequent) electric torque components for additional control features and sideward tower reactions are filtered out from (measured) feedback signals,

the actual electric torque $T_{\rm e}$ can be assumed approximately equal to $T_{\rm e}^*$ in eq.(2.8).

2.4 Rotor effective and uniform wind speed

In practice, the value of actual wind speed pertains to a specific point in time and position. The wind speed experienced by the turbine rotor, is converted to an effective aerodynamic torque at the main shaft. Therefore the 'rotor wide' wind speed in eq.(2.1) and eq.(2.2) is defined as 'rotor effective wind speed' [2]:

'a single point wind speed signal which will cause wind torque variations through rotor power and thrust coefficients, that will be stochastically equivalent to those calculated through blade element theory in a turbulent wind field'.

The stochastic wind speed signal is derived from the autopower spectrum of the longitudinal wind speed variations and lateral coherence in the rotor plane, according to IEC class IIA and turbulence intensity 16% [1]. The rotor effective wind speed signal has been normalised by the mean value of wind speed and comprises:

- tower shadow influences;
- wind shear variations;
- 0p mode of the turbulent windfield;
- 3p- and 6p effects of the rotationally sampled wind field.

Fig.(2.2) shows these components in detail during 20 seconds. In the upper plot of fig.(2.2), tower shadow influences are clearly visible as 3p periodical notches. Wind shear is nearly neglectable. The middle plot shows the 3p and 6p rotational wind field sampling effects of the blades. Because these effects considerably affect the rotor acceleration, incorporating them is significant to verify filtering performance during rotor speed control. The lower plot shows 'low frequent' wind speed variations (0p) determined by the stochastic properties of wind and turbulence intensity.

For simulation purposes the actual wind speed is determined from a priori calculated wind file comprising normalised periodical and turbulent components for actual rotor azimuth, $\Psi_{\rm r}$ and desired mean wind speed, $\overline{V}_{\rm w}$.

$$\begin{array}{rl} \Psi_{\rm r} = & \int^t \Omega_{\rm r} \cdot {\rm d}t \\ V_{\rm w} = & \overline{V}_{\rm w} \cdot [1 + v_{\rm w}^{\rm tur}(\Psi_{\rm r})] + \\ & \overline{V}_{\rm w} \cdot [1 + v_{\rm w}^{\rm tur_{0p}}(\Psi_{\rm r})] \cdot [v_{\rm w}^{\rm tow}(\Psi_{\rm r} {\rm mod} 2\pi) + v_{\rm w}^{\rm shr}(\Psi_{\rm r} {\rm mod} 2\pi)] \end{array} \tag{2.10}$$

In eq.(2.10), both tower shadow and wind shear variations are periodical effects in the range $[0, 2\pi]$ of the rotor azimuth, and scalable with 'rotor uniform wind', $V_{\rm w}^{\rm unif}$. Turbulence is approximately proportional with mean wind speed, $\overline{V}_{\rm w}$. In eq.(2.10), the components $v_{\rm w}^{\rm tur}$, $v_{\rm w}^{\rm tur_{0p}}$,$v_{\rm w}^{\rm tow}$ and $v_{\rm w}^{\rm shr}$ are normalised variations with respect to the mean windspeed $\overline{V}_{\rm w}$.

Finally, fig.(2.3) shows a simulation time serie of the rotor uniform wind speed and rotor effective wind speed, respectively.

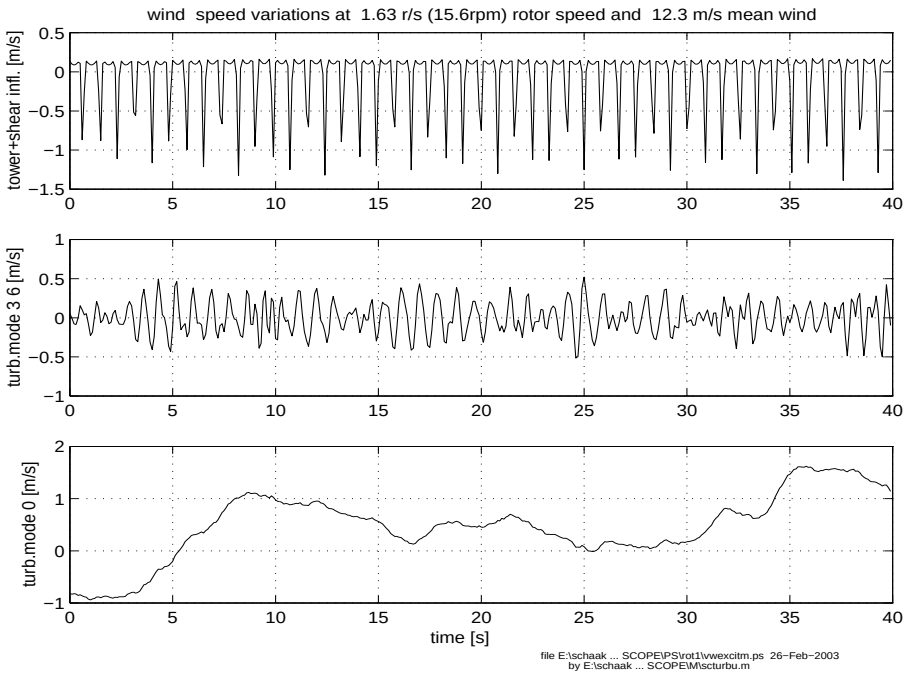

Figure 2.2: *Details of contributions to rotor effective windspeed; tower and shear, rotational sampling, 0p mode*

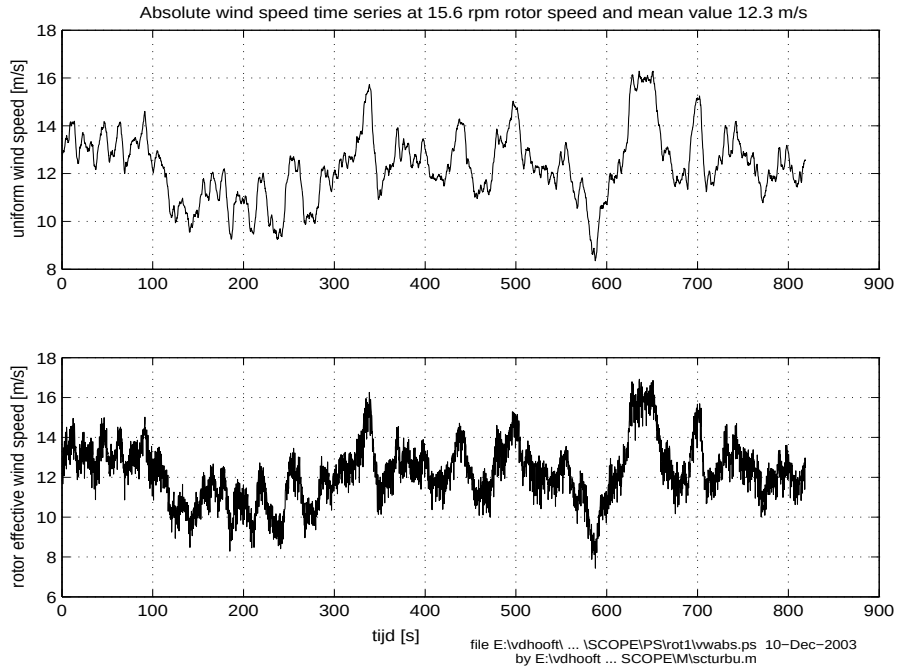

Figure 2.3: *Time series of uniform wind speed and rotor effective wind speed signals*

3 CONTROL STRUCTURE

In this chapter the basic control structure is described as a frame in which the proposed 'estimated wind speed feed forward' optimisation should act. At above rated wind speed conditions, power is usually controlled indirectly by rotor speed regulation (pitch control) and a stationary production curve (T_{e} = f(Ω_{r}), which aims constant rated power (generator control). Both pitch and electric torque control, as well as their mutual interaction, are explained for around and above rated wind speed conditions.

3.1 Rotor speed feedback control by pitch actuation

Operation of variable speed wind turbine can be divided into four operation modes: start-up, partial load control, full load control and shut-down. During start-up, pitch control is simply performed by moving the blades with constant speed ($\sim 1^{\mathrm{o}}/\mathrm{s}$) from feathering towards working position. Shut down, is performed by the turbine safety system.

The rotor speed feedback structure of pitch control is described for partial and full load operation. Special attention is paid to rotor speed filtering; this is not only an important issue for rotor speed control but for wind speed estimation as well chapter 4).

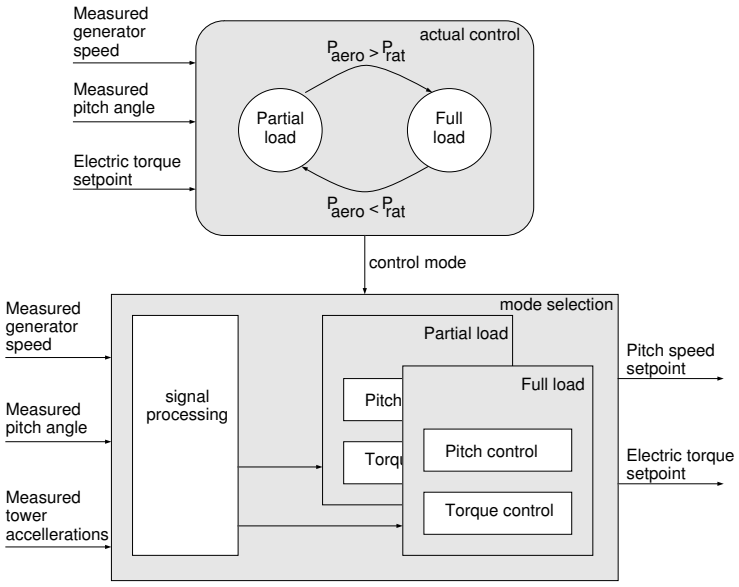

Figure 3.1: *Functional control structure*

The switching mechanism between partial and full load control will occur around rated condition and interacts with generator torque control, see subsection 3.2.2

3.1.1 Partial load control

Pitch control below rated conditions (partial load control) is simply achieved by maintaining the pitch angle in its working position (around 0 $^{\mathrm{o}}$), where the maximum aerodynamic efficiency is found (maximum value of C_{p}). In some situations the pitch angle is slightly controlled by a pitch angle servo to rotor speed dependent pitch angle setpoint values (noise, power, loads).

3.1.2 Full load pitch control

In fig.(3.2) the (functional) overall structure of the pitch controller at full load operation is shown [3]. The core is a control structure (PDC): feedback of the low pass filtered rotor speed

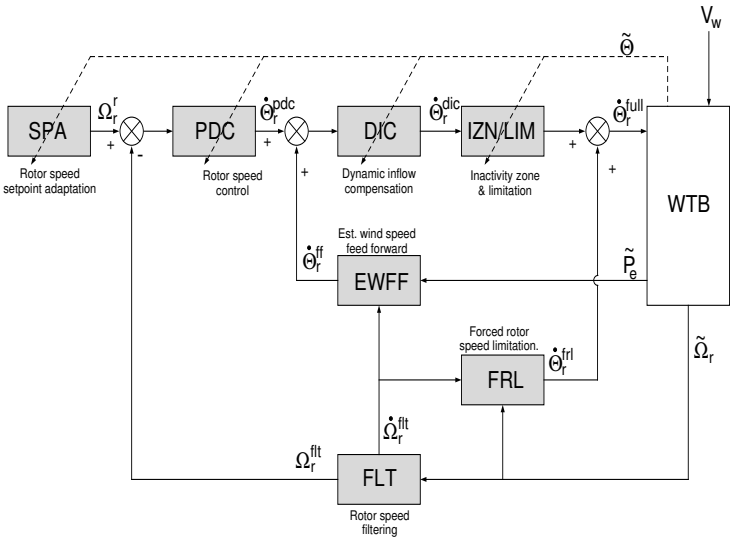

Figure 3.2: *functional overall structure of the pitch controller at full load operation*

($K_{\mathrm{P}}^{\Omega_{\mathrm{r}}} \cdot \tilde{\Omega}_{\mathrm{r}}^{\mathrm{f}}$, proportional part) and acceleration ($K_{\mathrm{P}}^{\Omega_{\mathrm{r}}} \cdot \dot{\tilde{\Omega}}_{\mathrm{r}}^{\mathrm{f}}$, differential part) back to a setpoint value of the pitching speed, $\dot{\theta}_{\Omega_{\mathrm{r}}}^{*}$. The pitch actuators of each blade will then set the pitch angle, θ simultaneously to a suitable position to regulate the rotor speed between its rated and maximum allowed value. The measured value of the rotor speed is filtered by a cascade filter (FLT, see next paragraph). Due to the heavily non linear character of the windturbine some non linear extensions are added to meet satisfied performance:

- linear controller gains have been scheduled dependent on the actual blade angle and the rotor speed; with gain scheduling the linear controller is adapted to the whole operation envelope of the wind turbine;
- an (scheduled) inactivity zone (IZN) with hysteresis, to avoid undesired pitch angle adjustments due to small controller corrections caused by noise, tower shadow, rotational sampling effects etc;
- rotor speed setpoint adaptation (< 0.5 rpm) at higher wind speed level (SPA), which supports the linear controller to avoid energy loss in case of sudden falling wind gusts (flywheel effect);
- pitching bounds are incorporated to limit the calculated pitch speed values (LIM);
- non linear compensation of the calculated pitching speed to cancel foreseen amplification due to 'dynamic inflow effects' (DIC, rotor wake effects).

To ensure no excess of maximum rotor speed a mechanism called 'forced rotor speed limitation' is able to overrule the closed loop rotor speed control loop by forcing the pitch angle quickly (4 dg/s) -but for a short period of time as possible- in vane direction as soon as the actual rotor speed exceeds a certain safety level ($\Omega_{\mathrm{r}}^{\max}$ - [0.5 rpm]) and is still accelerating;

In advance to chapter 4, the proposed 'estimated wind speed feed forward' is also introduced in fig.(3.2). It will add a non-linear control action to the pitching speed setpoint, $\dot{\theta}_{\hat{V}_{\mathrm{w}}}^{*}$ based on the reconstructed value of rotor effective wind speed, $\hat{V}_{\mathrm{w}}$.

Rotor speed filtering: The measured value of the rotor speed is filtered by a cascade filter. This filter shall suppress the following disturbing turbine effects sufficiently by means of digital filtering:

- 3p effects (section 2.4);
  - tower shadow;
  - 3p and 6p rotational sampling effects;
- collective lead-lag bending effects of the blades (section 2.2);
- sideward tower movements (section 2.3).

Because rotor acceleration is numerical calculated using the backward difference approach, all disturbances above the pitch control bandwidth has to be reduced to avoid amplification by the controller (differential) gain. In practice, it has been appeared that a reduction factor of al least 5 to 10 would be required for 3p frequencies and higher.

A cascade filter consisting of a fourth order inverse Chebychev low pass filter (3p effects), a fourth order elliptic band notch filter (collective lead-lag mode) and a second order elliptic band notch filter (sideward tower) as given in eq.(3.1) and specified in table(3.1) achieves sufficient reductions at least phase shift ($\sim 60^{\circ}$ at the controller Nyquist frequency $\omega_{\rm nq}$).

$$H^{\rm filt}_{\Omega_{\rm r}}(s) = H^{\rm filt,3p}_{\Omega_{\rm r}}(s) \cdot H^{\rm filt,col}_{\Omega_{\rm r}}(s) \cdot H^{\rm filt,tow}_{\Omega_{\rm r}}(s) \tag{3.1}$$

In fig.(3.3) the typical amplitude and phase characteristic of this filter is shown.

Table 3.1: *Rotor speed filter specifications*

Filtersection	1	2	3
Type	Invers Chebychev low pass	Elliptic band notch	Elliptic band notch
Behaviour	Low pass	Band notch	Band notch
Order	4	4	2
Reduction	30 dB	19 dB	29 dB
Pass ripple	-	1 dB	1 dB
cut-off	($\omega_0^{\rm 3p}$-0.3) $\rm rad/s$	-	-
notch	-	[0.625 1.125]$\omega_0^{\rm col}$	[0.85 1.15]$\omega_0^{\rm t}$

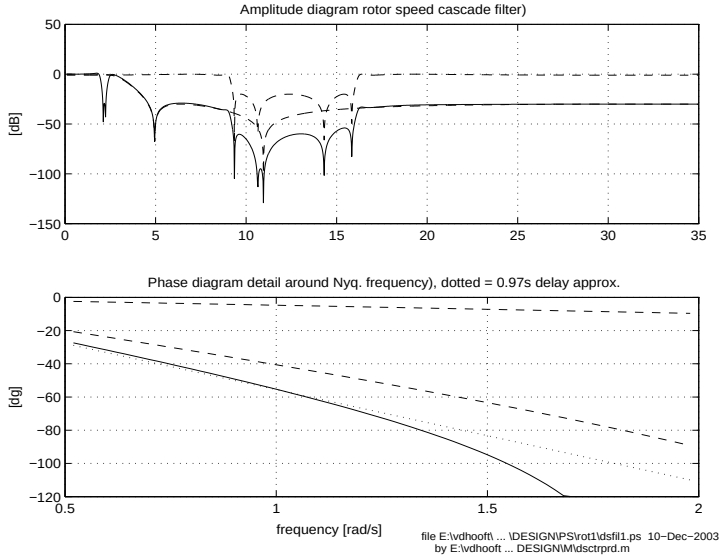

Figure 3.3: *Bode diagrams of rotor speed cascade filter (solid lines)*

3.2 Electric torque control

Electric torque control will primarily be used for power control (eq.(2.8)). Additionally, it is a quantity to optimise the transition zone around rated conditions between partial load control (below rated wind speed) and full load control (subsection 3.1).

3.2.1 Power production curve

In case of insufficient wind capture, constant rated power can not be maintained and transition to the optimum lambda curve is desired to improve aerodynamic efficiency. Reversely, as soon as there's wind capture excess during optimal lambda operation, transition to rated power is prefered to produce constant power and reduce loads. A linear transition curve connects the optimum lambda curve (below rated) with the constant power curve (above rated). In fig.(3.4) a typical generator production curve is shown. The dashed continuation of the constant power part, implies over torque at below rated rotor speed values: this will be valuable for transition optimisation purposes (subsection 3.2.2)

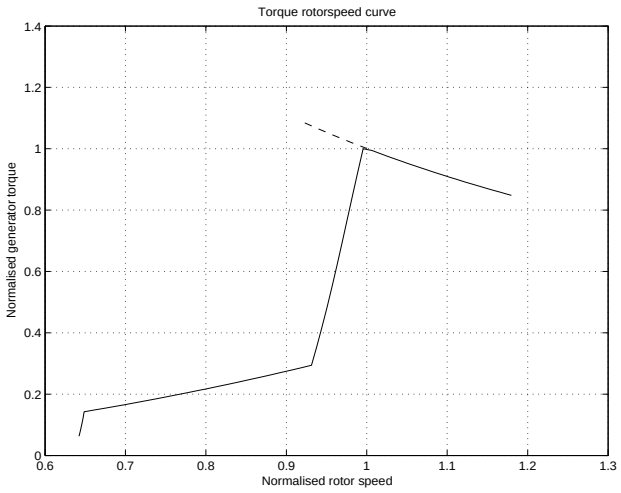

Figure 3.4: *Power production curve of a variable speed turbine*

3.2.2 Transition optimisation around rated

Optimisation around rated conditions can be achieved by using available overtorque capabilities of the electric actuation system and interaction between pitch and electric torque control [3] [4]:

- continuation of constant power curve for below rated rotor speed values, until a maximum allowable torque limit is reached
- simulataneous horizontal shifting of the transition curve to lower rotor speed;
- shifting back the torque transition curve towards its original position during partial load operation;
- for pitch control mode selection:
  - switch from constant power to optimum lambda operation only if pitch control has achieved its working position and the rotor speed, $\tilde{\Omega}_{\mathrm{r}}^{\mathrm{f}}$ is below rated value $\Omega_{\mathrm{r}}^{\mathrm{rat}}$;
  - switch back from optimum lambda to constant power simultaneously with pitch control (from partial to full load), if the rotor speed exceeds its rated value with a certain amount (hysteresis to avoid to many transitions);

4 ESTIMATED WIND SPEED FEED FORWARD

In this chapter, the power optimising control feature: 'feed forward of estimated wind speed' is introduced. In the first section the functional principle and requirements of this feature are discussed, while in the next sections two implementation possibilities are described: polynomial (see also [3]) and tabular implementation.

4.1 Principle

The principle of wind speed feed forward control is based on uniform wind speed estimation from aerodynamic torque for pitch actuation to achieve rated power. Strictly, it should be named as 'pseudo' feed forward control, because the wind speed is not directly fed in as a measured value, but is reconstructed from measurements and a priori knowledge of rotor behaviour ('feed back loop', see fig.(3.2)):

- low pass filtered measurements of rotorspeed ($\tilde{\Omega}_{\mathrm{r}}^{\mathrm{f}}$), pitch angle ($\tilde{\theta}^{\mathrm{f}}$) and electric power ($\tilde{P}_{\mathrm{e}}^{\mathrm{f}}$);
- aerodynamic behaviour: loss parameters ($\hat{C}_{\mathrm{c}}$ and $\hat{C}_{\Omega_{\mathrm{r}}}$), rotor torque coefficients ($\hat{C}_{\mathrm{q}}(\lambda,\theta)$), air density $\hat{\rho}_{\mathrm{air}}$;
- rotor parameters: rotordiameter ($\hat{R}_{\mathrm{b}}$), total inertia ($\hat{J}_{\mathrm{t}}$).

The low pass filtered rotor accelleration $\dot{\tilde{\Omega}}_{\mathrm{r}}^{\mathrm{f}}$ is numerically derived from $\tilde{\Omega}_{\mathrm{r}}$ and using similar low pass filtering. Using equal filtering for all measured quantities is an important issue to have the same phase lag. Aerodynamic losses are incorporated by estimation of torque losses, eq.(4.1)

$$\hat{T}_{\mathrm{l}} = \hat{C}_{\mathrm{c}} + \hat{C}_{\Omega_{\mathrm{r}}} \cdot \tilde{\Omega}_{\mathrm{r}} \tag{4.1}$$

The estimated wind speed feed forward structure consists of three sequential steps:

- reconstruction of aerodynamic torque, $\hat{T}_{\mathrm{a}}$;
- wind speed estimation, $\hat{V}_{\mathrm{w}}$;
- pitch speed setting, $\dot{\theta}^{*}_{\hat{V}_{\mathrm{w}}}$.

4.1.1 Reconstruction of aerodynamic torque

Using the (low frequency) power balance, aerodynamic torque ($\tilde{T}_{\mathrm{a}}$) can be reconstructed as given in eq.(4.2):

$$\tilde{T}_{\mathrm{a}} = \hat{J}_{\mathrm{t}} \cdot \dot{\tilde{\Omega}}_{\mathrm{r}}^{\mathrm{f}} + \left(\tilde{P}_{\mathrm{e}}^{\mathrm{f}} / \tilde{\Omega}_{\mathrm{r}}^{\mathrm{f}} \right) + \hat{T}_{\mathrm{l}} \tag{4.2}$$

in which $\hat{J}_{\mathrm{t}}$ has been defined in accordance to eq.(2.6). Reconstruction of aerodynamic is base on filtered values of rotor speed, -acceleration and electric torque.

If the dynamic behaviour of the electric torque actuator (generator including converter) are neglectable (bandwidth 5-10 times bandwidth low pass filtering), the power measurement can be avoided by replacing the second term of eq.(4.2) with the power production setpoint $T_{\mathrm{e}}^{*}(\Omega_{\mathrm{r}})$ (see section 2.3) .

Finally, it can be concluded that there's a 'simple' explicit relation for determination of $\hat{T}_{\mathrm{a}}$.

4.1.2 Wind speed estimation

Due to the 'absence' of high order components ($\omega > \omega_0^{3p}$) in the reconstructed aerodynamic torque $\hat{T}_a$, the estimated wind speed value $\hat{V}_w$ will be a (delayed) approximation of the fictive rotor uniform wind speed, V_w^{unif}(section 2.4). The relationship between $\hat{T}_a$ and $\hat{V}_w$ is described in accordance with eq.(2.1):

$$\hat{C}_q(\tilde{\theta}^f, \hat{\lambda}) \cdot \tfrac{1}{2}\hat{\rho}_{air}\pi\hat{R}_b^3 \cdot (\hat{V}_w)^2 = \hat{T}_a \tag{4.3}$$

In eq.(4.3), fore-aft tower displacements, $\dot{x}_{nd}$ are taken for granted. If any relevance, $\hat{V}_w$ can be compensated for these fore-aft movements afterwards, provided that the tower top acceleration $\ddot{\tilde{x}}_{nd}$ is measured.

Because $\hat{C}_q$ is dependent of the tip speed ratio $\hat{\lambda}$, eq.(4.4), there's an implicit relationship between $\hat{T}_a$ and $\hat{V}_w$.

$$\hat{\lambda} = \frac{\tilde{\Omega}_r^f \cdot \hat{R}_b}{\hat{V}_w} \tag{4.4}$$

In the operation range of the turbine, the relation T_a= f(V_w) is not always a function in mathematical sense. In other words, there's more than one valid solution of wind speed $\hat{V}_w$ for a collection of operation points determined by $\hat{T}_a$, $\tilde{\Omega}_r$ and $\tilde{\theta}$. This happens specifically for rotor speeds at small pitch angles (see fig.(4.1)). At higher pitch angles the relation T_a = f(V_w)

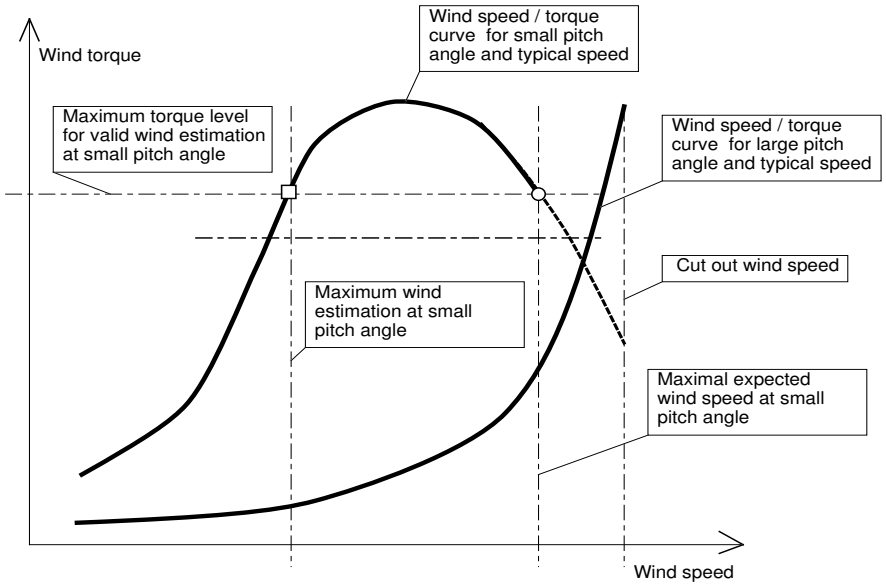

Figure 4.1: *Relationship between wind torque and wind speed for estimation procedure for certain values of pitch angle, wind torque and rotor speed*

shows unique solutions. The physical meaning of two solutions is found in the nature of air flow: the 'low wind speed solution' implies attached flow, while the 'high wind speed solution' implies stall or turbulent flow. Stall solutions will be left out of consideration, the special cases of stall conditions for a 'pitch to vane turbine' are ignored and interpreted as 'invalid solution'.

By ignoring 'stall' solutions, $\hat{T}_a$ = f($\hat{V}_w$) shows monotonic behaviour for all relevant values of $\tilde{\theta}$ and $\tilde{\Omega}_r$. Therefore, a unique solution for $\hat{V}_w$ can be found from eq.(4.2) and eq.(4.3) by solving the implicit relationship; this is rather complex (subsection 4.3.1 and subsection 4.4.1).

4.1.3 Pitch speed setting

The estimated wind speed will be used to realise an additional pitch control action, which optimises the turbine power production and improves its behaviour at sudden wind gusts. A target pitch angle value $\theta^*_{\hat{V}_w}$ is aimed to maintain stationary rated power production. It appears to have a relation with the estimated wind speed, $\hat{V}_w$, and the measured rotor speed $\tilde{\Omega}^f_r$ by eq.(4.5)

$$\hat{C}_p(\theta^*_{\hat{V}_w}, \hat{\lambda}) \cdot \tfrac{1}{2}\hat{\rho}_{air}\pi\hat{R}^2_b \cdot (\hat{V}_w)^3 = P^{rat}_a \tag{4.5}$$

Determination of $\theta^*_{\hat{V}_w}$ from eq.(4.5) will be complicated because of the implicit relationship with $\hat{V}_w$. Although, this can be solved off-line numerically (subsection 4.3.2 and subsection 4.4.2).

The pitch speed setpoint, $\dot{\theta}^*_{\hat{V}_w}$ for wind speed changes is determined from eq.(4.6)

$$\dot{\theta}^*_{\hat{V}_w} = (\theta^*_{\hat{V}_w})'_{\hat{V}_w} \cdot \dot{\hat{V}}_w \tag{4.6}$$

in which the non-linear scaling facotr $(\theta^*_{\hat{V}_w})'_{\hat{V}_w}$ can be derived from the solution of eq.(4.5).

From control viewpoint, eq.(4.6) implies a D-action from estimated wind speed to pitch speed, including a non linear gain to maintain rated power. To comply with stability and numerical noise restrictions, a scale factor $K^{\hat{V}_w}_D$ and moderate differentiation $\tau^{\hat{V}_w}_D$ is introduced (in Laplace domain):

$$H^c_{\hat{V}_w}(s) = \frac{\dot{\theta}^*_{\hat{V}_w}(s)}{\hat{V}_w(s)} = (\theta^*_{\hat{V}_w})'_{\hat{V}_w} \cdot K^{\hat{V}_w}_D \cdot \frac{\tau^{\hat{V}_w}_D \cdot s}{1 + \tau^{\hat{V}_w}_D \cdot s} \tag{4.7}$$

Due to the high sensitivity in the wind acceleration, the maximum value is usually limited to $4^o/s$ to avoid nervous pitch control actions. In the frequency domain, the moderate D-action acts as a first order high pass filter with gain $K^{\hat{V}_w}_D$ and cut-off frequency at $1/\tau^{\hat{V}_w}_D$. In combination with the low pass filtered rotor speed and acceleration (eq.(3.1)) this series behaviour results in a bandpass characteristic. Therefore, the value of $1/\tau^{\hat{V}_w}_D$ should:

- be lower than ω^{3p}_0 (and the collective mode ω^{col}_0);
- give sufficient passing bandwidth;
- not affect the very low (stationary) frequency behaviour.

This results usually in a typical value of between 0.5-1s. The scale factor $K^{\hat{V}_w}_D$ is more arbitrary, but for stability reasons a value greater than unity is not allowed (0.5 - 0.8).

Two conditional rules are added to optimise the co-operation between estimated wind speed feed forward control and rotor speed control; pitch speed contributions

- in vane direction are only effectuated if $\tilde{\Omega}^f_r > \Omega^{max}_{r,\hat{V}_w}$;
- in work direction are only effectuated if $\tilde{\Omega}^f_r < \Omega^{min}_{r,\hat{V}_w}$;

Typical values for $\Omega^{max}_{r,\hat{V}_w}$ and $\Omega^{min}_{r,\hat{V}_w}$ are usually (Ω^{rat}_r +1 rpm) and Ω^{rat}_r .

From viewpoint of stability ‘estimated wind speed feed forward control’ adds an additional higly non-linear DD-control action to rotor speed feedback (‘jerk control’): the change of estimated wind speed means the change of the rotor acceleration term $\hat{J}_t \cdot \dot{\tilde{\Omega}}^f_r$ which implies DD-control.

4.2 Implementation

Implementation of 'the estimated wind speed feed forward' principles in the pitch control algorithm can be done either by a *polynomial approach* (section 4.3) or a *tabular approach* (section 4.4).

The polynomial implementation approach means that the implicit relations , eq.(4.3) and eq.(4.5) would be *approximated* by means of (multi-dimensional) polynomial fits. The determination of estimated wind speed, $\hat{V}_{\mathrm{w}}$, from reconstructed aerodynamic torque, $\hat{T}_{\mathrm{a}}$, should be done each control cycle (on-line) by an iterative method as Newton Raphson. Determination of the non-linear feed forward gain to achieve rated power, $(\theta^{*}_{\hat{\mathrm{V}}_{\mathrm{w}}})'_{\hat{\mathrm{V}}_{\mathrm{w}}}$, can be done prior (off-line) to the implementation of the algorithm.

The tabular approach implies that the implicit relations are *solved* prior to implementation of the algorithm (off-line). The numerically found solutions, are stored in (multi-dimensional) tables, in which the on-line control algorithm will search for matching solutions, dependent of the actual operation point. Increase of accuracy and decrease of the table grid density (size), can be achieved by on-line linear interpolation.

For the following reasons the tabular approach is preferable with respect to the polynomial approach (these arguments will become clear in the next sections):

- the implementation code is simple and robust;
- no intensive calculations (dedicated hardware);
- no danger for faulty solutions outside the operation area;
- no watching mechanisms to check convergence or to validate solutions;
- no initialising mechanism;

The only drawback of tabular implementation will be the size of tables, but memory is no longer an issue nowadays. Therefore, the polynomial implementation is described only in general terms in section 4.3, while the tabular implementation will be explained in more detail in section 4.3.

4.3 Polynomial implementation

The next two sections will describe the polynomial implementation approach in two steps, respectively the estimation of uniform wind speed and the non-linear gain of the 'feed forward' mechanism.

4.3.1 Wind speed estimation

The unique solution for $\hat{V}_{\mathrm{w}}$ from eq.(4.2) and eq.(4.3) is found by using the quick converging numeric iterative method of Newton-Raphson ('gradient method'):

$$\hat{V}_{\mathrm{w}}^{(\mathrm{k})} = \hat{V}_{\mathrm{w}}^{(\mathrm{k}-1)} - \frac{\left(\tilde{T}_{\mathrm{a}} - \hat{T}_{\mathrm{a}}^{(\mathrm{k}-1)}\right)}{\left(\frac{\mathrm{d}\hat{T}_{\mathrm{a}}}{\mathrm{d}\hat{V}_{\mathrm{w}}}\right)_{\hat{V}_{\mathrm{w}}^{(\mathrm{k}-1)}}} \tag{4.8}$$

The superscript (k) and (k-1) in eq.(4.8), represents time-discrete instances for the actual and old value, respectively. Usually, the iteration loop will be interrupted after 2 or 3 steps because of sufficient accuracy regarding $|\tilde{T}_{\mathrm{a}} - \hat{T}_{\mathrm{a}}|$ and $|\hat{V}_{\mathrm{w}}^{(\mathrm{k})} - \hat{V}_{\mathrm{w}}^{(\mathrm{k}-1)}|$.

The aerodynamic torque coefficients in eq.(4.3) are off-line fitted to a 2D-polynomial function:

$$\hat{C}_{\mathrm{q}}(\tilde{\theta}^{\mathrm{f}}, \hat{\lambda}^{-1}) = \sum_{\mathrm{i}=1}^{\mathrm{N}_{\theta}+1} \sum_{\mathrm{j}=1}^{\mathrm{N}\Omega_{\mathrm{r}}+1} C_{\mathrm{C_q}}(i,j) \cdot \theta^{(j-1)} \cdot \lambda^{-(i-1)} \tag{4.9}$$

The maximum allowable aerodynamic torque levels for wind speed estimation, $T^{\max}_{\hat{V}_w}(\tilde{\theta},\tilde{\Omega}_r)$ which checks on 'stall' solutions, are also fitted off-line to a 2D-polynomial function:

$$T^{\max}_{\hat{V}_w}(\tilde{\theta}^f,\tilde{\Omega}^f_r) = \sum_{i=1}^{N_{\Omega_r}+1}\sum_{j=1}^{N_\theta+1} C_{T^{\max}_{\hat{V}_w}}(i,j)\cdot\theta^{(j-1)}\cdot\Omega_r^{(i-1)} \tag{4.10}$$

To avoid to much transitions between the valid/invalid states, the actual aerodynamic torque limit for wind speed estimation is low pass filtered (10s) and switch hysteresis (+/- 5%) is applied.

To ensure numeric convergence (start-up, invalid solution), a favourable initial wind speed estimation ($\hat{V}^{ini}_w$) is calculated from a specific 2D-polynomial function,

$$\hat{V}^{ini}_w(\tilde{\theta}^f,\tilde{\Omega}_r f) = \sum_{i=1}^{N_{\Omega_r}+1}\sum_{j=1}^{N_\theta+1} C_{\hat{V}^{ini}_w}(i,j)\cdot\theta^{(j-1)}\cdot\Omega_r^{(i-1)} \tag{4.11}$$

This polynomial is also calculated off-line and is based on sufficient torque to wind speed sensitivity for all relevant operation points.

Fig.(4.2) shows the theoretical and fitted results of wind speed estimation for typical values of pitch angle, rotor speed and allowed aerodynamic torque range within the operation range. Both theoretical and fitted results are almost equal. The 'asterix' markers shows the initial operation points, from which convergence is guaranteed if wind speed estimation should start-up from scratch.

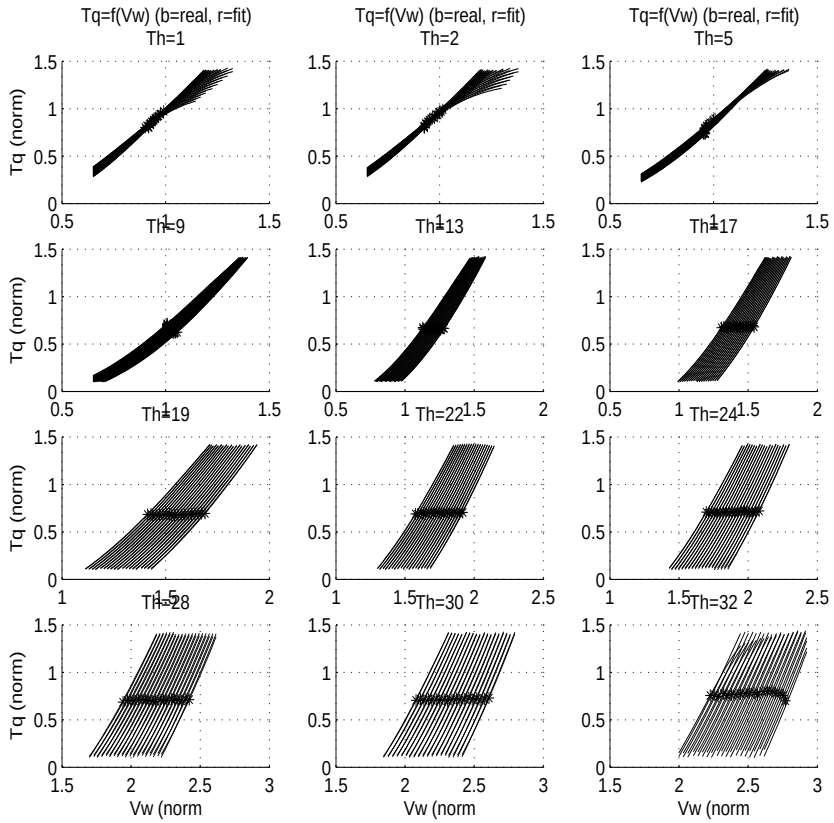

Figure 4.2: *Theoretical and fitted results of wind speed estimation from aerodynamic torque for the wind turbine operation range; asterix markers imply initial start values*

In practice all 2D polynomials are of degree 4 and their actual value is determined by using filtered values.

4.3.2 Pitch speed effectuation

Determination of $\theta^*_{\hat{V}_w}$ from eq.(4.5) will be complicated because of the implicit relationship with $\hat{V}_w$. Although, this can be solved off-line numerically,

The numerical solution for $\theta^*_{\hat{V}_w}$, results in a 2D-polynomial function (eq.(4.12), V_w^{-1} dependancy)

$$\theta^*_{\hat{V}_w}(\hat{V}_w, \tilde{\Omega}_r) = \sum_{i=1}^{N_{V_w}+1} \sum_{j=1}^{N_{\Omega_r}+1} C_{\theta^*_{\hat{V}_w^{-1}}}(i,j) \cdot \Omega^{(j-1)} \cdot V_w^{-(i-1)} \tag{4.12}$$

The pitch speed setpoint, $\dot{\theta}^*_{\hat{V}_w}$ for wind speed changes is determined from eq.(4.6), in which the feed forward gain factor $(\theta^*_{\hat{V}_w})'_{\hat{V}_w}$ can be found from eq.(4.12) by convenient differentiation of polynomial power functions:

$$(\theta^*_{\hat{V}_w})'_{\hat{V}_w}(\hat{V}_w, \tilde{\Omega}^f_r) = \sum_{i=1}^{N_{V_w}+1} \sum_{j=1}^{N_{\Omega_r}+1} -(i-1) \cdot C_{\theta^*_{\hat{V}_w^{-1}}}(i,j) \cdot \Omega^{(j-1)} \cdot V_w^{-i}. \tag{4.13}$$

Fig.(4.3) shows the feed forward gain factor. (eq.(4.13))

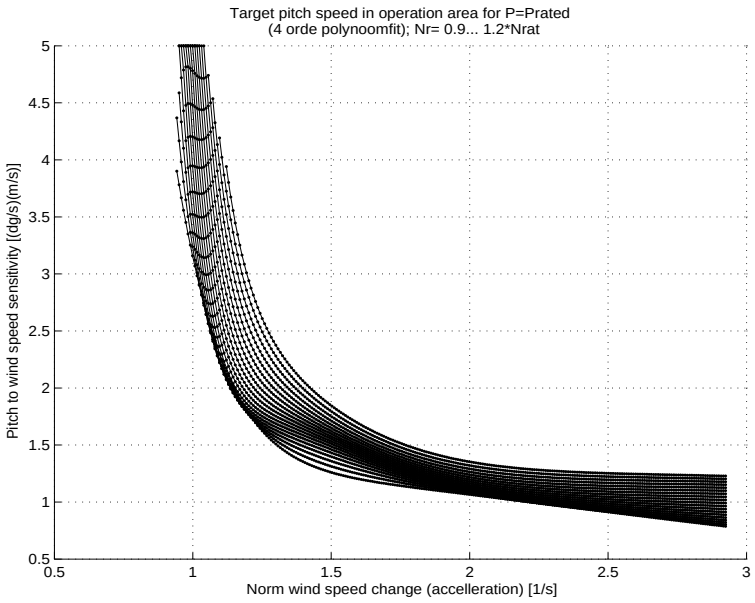

Figure 4.3: *(Polynomial) feed forward gain factor for wind speed variations (accelleration) within the wind turbine operation range*

The maximum sensitivity is limited to a maximum allowable value ($4^o/(m/s)$) to avoid extreme pitch actuation.

The degree of this 2D polynomial expression will practically be, N_{V_w}=4, N_{Ω_r}=4. The actual value of this sensitivity gain factor (scheduling) will be determined by using the estimated wind speed, $\hat{V}_w$ value as determined from eq.(4.8) and the filtered rotor speed $\tilde{\Omega}^f_r$.

4.4 Tabular implementation

The next sections will explain the tabular implementation approach in respectively two steps: the estimation of uniform wind speed, the non-linear gain of the 'feed forward' mechanism. Finally, for use in the (cyclic) control algorithm, a four step (on-line) algorithm for operation point determination, quick tabular search, interpolation and effectuation is described.

4.4.1 Wind speed estimation

In case of tabular implementation, determination of the estimated wind speed $\hat{V}_{\rm w}$ is done off-line by solving the implicit relation as given by eq.(4.2) and eq.(4.3). A benefit of this approach is the possibility to use advanced numerical methods to solve this complicated relation and only for relevant operation points. The 'estimated' wind speed solutions are stored in a three dimensional table $f^{\rm TAB}_{\hat{\rm V}_{\rm w}}$ which has been created by three range vectors: $\theta^{\rm RNG}$, $T^{\rm RNG}_{\rm a}$ and $\Omega^{\rm RNG}_{\rm r}$.

$$\hat{V}_{\rm w} = f^{\rm TAB}_{\hat{\rm V}_{\rm w}}\left(\theta^{\rm RNG}, T^{\rm RNG}_{\rm a}, \Omega^{\rm RNG}_{\rm r}\right), \tag{4.14}$$

For each actual operation point ($\tilde{\theta}^{\rm f}$, $\hat{T}_{\rm a}$, $\tilde{\Omega}^{\rm f}_{\rm r}$) , the pertaining wind speed $\hat{V}_{\rm w}$ can be retrieved on-line, by a quick search and interpolation algorithm (subsection 4.4.3).

The table of eq.(4.14) is build by performing the following steps off-line in advance:

1. define operation area for aerodynamic torque, pitch angle and rotor speed:
   (a) range limits (table range) [1];
   (b) number of levels (table grid density) [2];
   (c) equidistant distributed table grid;
2. find, within this operation range, the two nearest unique tip-speed ratio values, $\hat{\lambda}$, which deals with both equations (equilibrium) eq.(4.2) and eq.(4.3);
   (a) increase accuracy in this interval by linear interpolation;
   (b) if a unique solution is not found, then temporarily mark this operation point in the table;
3. check the table on monotonicity, omit and temporarily mark non-monotonic points in the table;
4. extrapolate all marked operation points in order to fill up the whole table with relevant values.

In fig.(4.4), the operation area for wind speed estimation is shown. The asterix points are operation points where unique solutions were found, while the dotted points in the upper right and lower left corner are (additional) extrapolated operation points. The 'dark' cloud in the figure illustrates operation points from time domain simulation at five different mean wind speed levels from $V^{\rm rat}_{\rm w}$ through $V^{\rm co}_{\rm w}$. It is proved that the operation range covers the turbine operation range sufficiently.

The wind speed table $f^{\rm TAB}_{\hat{\rm V}_{\rm w}}$ as well as the operation range vectors $\theta^{\rm RNG}$, $T^{\rm RNG}_{\rm a}$ and $\Omega^{\rm RNG}_{\rm r}$ will be stored for on-line use. It should be guaranteed that the range vectors are monotonic and increasing.

[1] Operation range limits are usually defined relative to their rated values, practical ranges are respectively: [0.4 .. 1.5]·$T^{\rm rat}$, [0 .. 32]$^{\rm o}$, [-1 .. 2]rpm +$\Omega^{\rm rat}_{\rm r}$

[2] Practical grid densities are respectively: 6 torque levels, 10 pitch angle levels and 6 rotor speed levels; ; this results in a wind speed table of 360 elements.

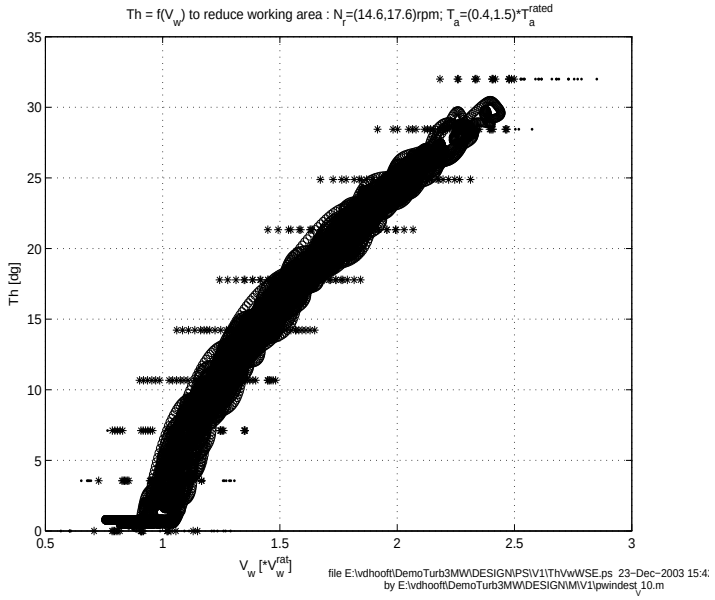

Figure 4.4: *(Tabular) operation area for wind speed estimation*

4.4.2 Pitch speed effectuation

Similar to subsection 4.4.1, the implicit relationship between the pitch angle reference value $\theta^*_{\hat{V}_w}$ and estimated wind speed $\hat{V}_w$, under the restriction of constant rated power (eq.(4.5)), can be solved off-line by using more advanced numerical methods within the turbine operation area. After post-processing these solutions, pitch speed feed forward gain values are stored in a two dimensional table $f^{TAB}_{\dot{\theta}^*_{\hat{V}_w}}$, which has been created by two range vectors: $\hat{V}_w^{RNG}$ and Ω_r^{RNG}

$$(\theta^*_{\hat{V}_w})'_{\hat{V}_w} = f^{TAB}_{\dot{\theta}^*_{\hat{V}_w}} \left(\hat{V}_w^{RNG} \Omega_r^{RNG} \right) . \tag{4.15}$$

For each operation point ($\hat{V}_w$, $\tilde{\Omega}_r^f$) , the pertaining feed forward gain factor $(\theta^*_{\hat{V}_w})'_{\hat{V}_w}$ can be retrieved on-line, by a quick search and interpolation algorithm (subsection 4.4.3).
The table of eq.(4.15) is build by performing the following steps off-line:

1. define operation area for estimated wind speed (initial) and rotor speed:
   (a) range limits (table range) [3];
   (b) number of levels (table grid density) [4];
   (c) logarithmic distributed table grid ;
2. find, within this operation range, the two nearest unique pitch angle values, $\theta^*_{\hat{V}_w}$, which deals with (equilibrium) eq.(4.5):
   (a) increase accuracy in this interval by linear interpolation;
   (b) if a unique solution is not found, then temporarily mark this operation point in the table;

[3] Operation range limits are usually defined relative to their rated values, practical ranges are respectively: [0.7 .. 2.5]·V_w^{rat}, [-1 .. 2]rpm +Ω_r^{rat}

[4] Practical grid densities are respectively: 30 wind speed levels and 6 rotor speed levels; this results in a feed forward gain table of 180 elements.

3. determine a polynomial fit for all (non-marked) solutions $\theta^*_{\hat{V}_w}$ for $\frac{1}{\hat{V}_w^{RNG}}$ and Ω_r^{RNG} (similar to eq.(4.12));
4. derive a polynomial expression for $(\theta^*_{\hat{V}_w})'_{\hat{V}_w}$ by adaptation of the polynomial coefficients and power degree (similar to eq.(4.13)); evolve this polynomial expression for the operation range back to a high resolution 2D table;
5. limit the table values to maximum and minimum allowable gain values ($4\,^{o}$/(m/s), 1^{o}/(m/s))
6. compose a new, more effective distributed wind speed range vector
7. interpolate an effective 2D table $f^{TAB}_{\dot{\theta}^*_{\hat{V}_w}}$, created by the new range vector $\hat{V}_w^{RNG}$ and the range vector Ω_r^{RNG} from the high resolution 2D table by interpolation.

It should be guaranteed that the range vectors are monotonic and increasing. Fig.(4.5) shows the feed forward gain factor, obviously this figure is similar to the polynomial approach of fig.(4.3).

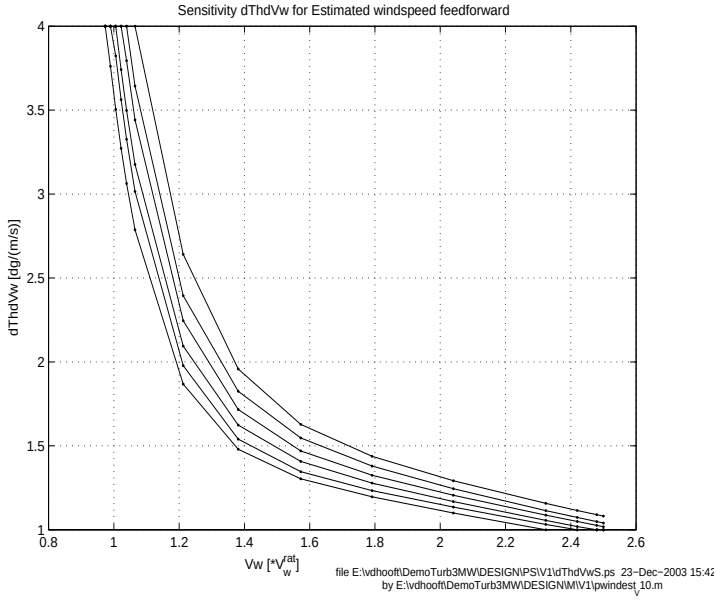

Figure 4.5: *(Tabular) feed forward gain factor for wind speed variations (accelleration) within the wind turbine operation range*

The dots are stored points in the table $f^{TAB}_{\dot{\theta}^*_{\hat{V}_w}}$, the dedicated distribution at the high sensitivity slope is clearly visible: only 70 values has given sufficient performance!

4.4.3 Control algorithm for feed forward of estimated wind speed

The stored solutions of the implicit functions for estimated wind speed, $\hat{V}_{\mathrm{w}}$, and the feed forward gain factor $(\theta^{*}_{\hat{V}_{\mathrm{w}}})'_{\hat{V}_{\mathrm{w}}}$ are stored in two tables, respectively:

- The 3D wind speed table $f^{\mathrm{TAB}}_{\hat{V}_{\mathrm{w}}}$ and the pertaining operation range vectors θ^{RNG} , $T^{\mathrm{RNG}}_{\mathrm{a}}$ and $\Omega^{\mathrm{RNG}}_{\mathrm{r}}$ (subsection 4.4.1);
- The 2D feed forward gain factor table $f^{\mathrm{TAB}}_{\theta^{*}_{\hat{V}_{\mathrm{w}}}}$ and the pertaining operation range vectors $\hat{V}^{\mathrm{RNG}}_{\mathrm{w}}$ and $\Omega^{\mathrm{RNG}}_{\mathrm{r}}$ (subsection 4.4.2).

An on-line algorithm will find matching solutions, dependent of the actual operation point. This will be achieved in four steps:

- actual operation point determination;
- quick tabular search algorithm;
- interpolation algorithm;
- effectuation of wind speed feed forward control.

Actual operation point determination: To determine the actual operation point, three actual quantities should be available: pitch angle, θ^{f} , rotor speed $\Omega^{\mathrm{f}}_{\mathrm{r}}$ and reconstructed aerodynamic torque $\tilde{T}_{\mathrm{a}}$. All quantities should be equally low pass filtered to avoid any shift in phase. Reconstruction of aerodynamic torque has been discussed in detail in subsection 4.1.1.

Quick tabular search algorithm: Based on the actual value of a quantity and its accompanying range vector (θ^{RNG} , $T^{\mathrm{RNG}}_{\mathrm{a}}$, $\Omega^{\mathrm{RNG}}_{\mathrm{r}}$ or $\hat{V}^{\mathrm{RNG}}_{\mathrm{w}}$), the quantity interval, in which the actual value is situated, can be found by a quick tabular search algorithm. Because this shall be done three times for wind speed estimation and two times for the feed forward gain factor in each control cycle, a subroutine (MATLAB function: ECNIXSEARCH.M) as specified below will facilitate this. The function code of ECNIXSEARCH is based on a simple linear search method.

ECNIXSEARCH()	:	quick search of argument interval indici in list
Call	:	[ixHi,ixLo,Status] = ecnixsearch(ArgSearch, IntList, ixOld)
Input	:	ArgSearch = search argument IntList = list with a number of discrete interval levels (>1) ixOld = index of previous (ixHi) argument
Output	:	ixLo = lower interval index in list ixHi = higher interval index in list Abort = quality of search result: +1 (succesfull), -1 (out of search range)
Description	:	ECNIXSEARCH is a quick algorithm to find both the lower and higher index of an demanded argument in a given list containing interval levels.Two input arguments (ArgSearch, IntList) are mandatory, but for quick search it is recommended to use the optional input argument ixOld. One output argument (ixHi), is mandatory while ixLo and Status are optionally given if requested as output argument in the function call.

If the actual value is outside the range vector, then the algorithm will result in the first/last interval, of the range vector, while the status-flag is set to -1.

Interpolation algorithm: Increase of the accuracy of the matching function value ($\hat{V}_{\mathrm{w}}$, $(\theta^{*}_{\hat{V}_{\mathrm{w}}})'_{\hat{V}_{\mathrm{w}}}$), will be achieved by linear interpolation between the determined range vector intervals. Fig.(4.6) illustrates the 3D interpolation approach (obvioulsy, 2D interpolation will be a simplification of 3D interpolation).

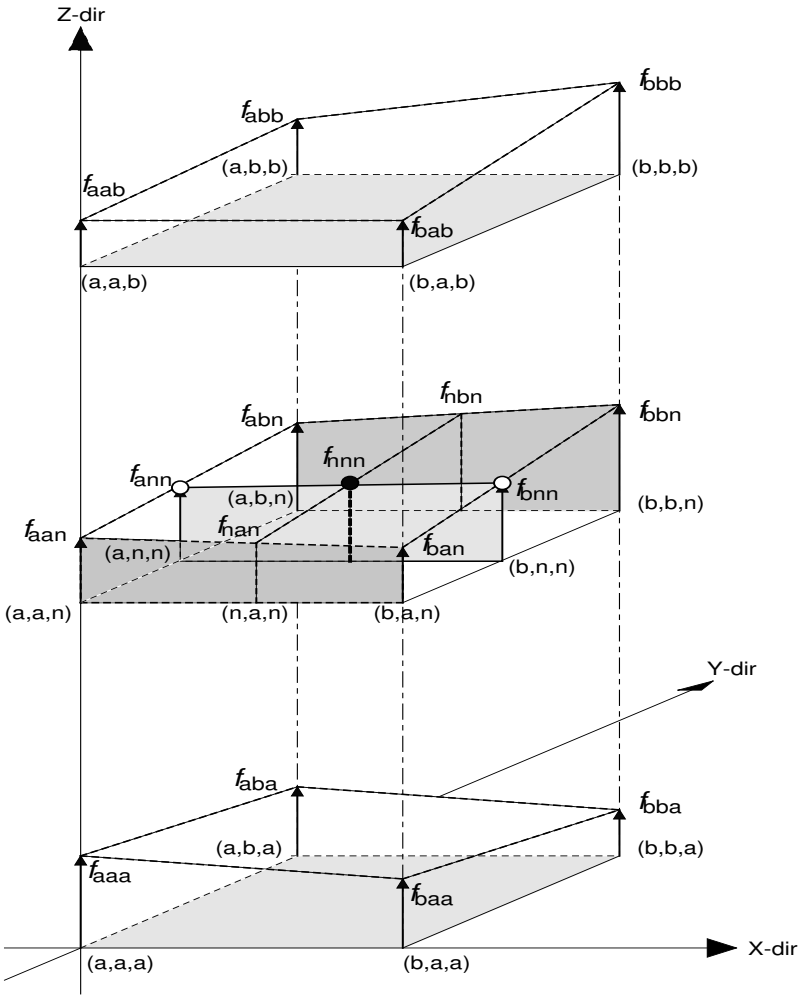

Figure 4.6: *Representation of the interpolation approach*

Mathematically considered , one actual function value f_{nnn} should be linear interpolated in a 4D space, consisting of three arguments (x, y, z) at the interval values $[a, b]$ and their pertaining function values (f). To achieve this, the interpolation process is broken down into three separated sub-processes for each argument (x, y, z) separately):

1. Interpolation sub-process of z-argument:

   (a) a space between two 3D bodies at z_{a} and z_{b} is proposed;

   (b) an actual function surface f_{xyn} is found by *four line interpolations* to find f_{aan}, f_{abn}, f_{ban} and f_{bbn} ;

2. Interpolation sub-process of y-argument:

   (a) a space between two surfaces y_{a} and y_{b} at z_{n} is proposed (dark shadowed);

   (b) an actual function line f_{xnn} is found by *two line interpolations* to find f_{ann}, f_{bnn} (light shadowed);

3. Interpolation sub-process of x-argument:

   (a) a 'space' between two lines x_{a} and x_{b} , at z_{n} and y_{n} , is proposed (white bullets);
   (b) the desired function point f_{nnn} is found by *one line interpolation*;

The algorithm as described above can be implemented straightforward as given in eq.(4.16)

$$\begin{aligned} f_{\mathrm{aan}} &= f_{\mathrm{aaa}} + \gamma \cdot (f_{\mathrm{aab}} - f_{\mathrm{aaa}}) \\ f_{\mathrm{abn}} &= f_{\mathrm{aba}} + \gamma \cdot (f_{\mathrm{abb}} - f_{\mathrm{aba}}) \\ f_{\mathrm{ban}} &= f_{\mathrm{baa}} + \gamma \cdot (f_{\mathrm{bab}} - f_{\mathrm{baa}}) \\ f_{\mathrm{bbn}} &= f_{\mathrm{bba}} + \gamma \cdot (f_{\mathrm{bbb}} - f_{\mathrm{bba}}) \\ \\ f_{\mathrm{ann}} &= f_{\mathrm{aan}} + \beta \cdot (f_{\mathrm{abn}} - f_{\mathrm{aan}}) \\ f_{\mathrm{bnn}} &= f_{\mathrm{ban}} + \beta \cdot (f_{\mathrm{bbn}} - f_{\mathrm{ban}}) \\ \\ f_{\mathrm{nnn}} &= f_{\mathrm{ann}} + \alpha \cdot (f_{\mathrm{bnn}} - f_{\mathrm{ann}}) \end{aligned} \tag{4.16}$$

where :

$$\begin{aligned} \gamma &= (\min(z_{\mathrm{b}}, \max(z_{\mathrm{a}}, z_{\mathrm{a}})) - z_{\mathrm{a}})/(z_{\mathrm{b}} - z_{\mathrm{a}}) \\ \beta &= (\min(y_{\mathrm{b}}, \max(y_{\mathrm{a}}, y_{\mathrm{a}})) - y_{\mathrm{a}})/(y_{\mathrm{b}} - y_{\mathrm{a}}) \\ \alpha &= (\min(x_{\mathrm{b}}, \max(x_{\mathrm{a}}, x_{\mathrm{a}})) - x_{\mathrm{a}})/(x_{\mathrm{b}} - x_{\mathrm{a}}) \end{aligned} \tag{4.17}$$

The multipliers α, β and γ in eq.(4.17) are clipped between the table values to avoid extrapolations outside the table.

To validate the proposed algorithms both the uniform wind speed and the feed forward gain factor, have been reconstructed from previous time domain simulations by using the resulting 'measurements' of rotor speed, pitch angle and electric power. These results are shown in fig.(4.7). The top window shows both the uniform wind speed $V_{\mathrm{w}}^{\mathrm{unif}}$ and its estimated approximation $\hat{V}_{\mathrm{w}}$. There's hardly any difference between both wind speeds; this excellent performance can be expected due to exact approximations of parameters and non-linearities, although it proves the algorithms as proposed in subsection 4.4.3 and (4.4.1). The lower three windows show the proper working of the quick search and linear interpolation algorithm. The horizontal dashed lines represents the linear distributed grid densities of the range vectors, for the pitch angle, aerodynamic torque and rotor speed respectively 10, 6 and 6. The staircase lines depicts lower and upper level of the interval, which was found by the search algorithms, while the smooth lines are the actual values. The good performance, for a relative number of grid levels, is attributed to the apparently piecewise linear behaviour of these signals.

The resulting feed forward gain factor is shown in the fifth window, its smooth behaviour satisfies and the varying values are caused by the operation area just above rated (steep edge of the slope in fig.(4.5). The two windows at the bottom show again proper working of the search and interpolation algorithms. The dedicated grid distribution of the (estimated) wind speed is clearly visible at low wind speed values.

Effectuation of wind speed feed forward control: Now both the estimated wind speed $\hat{V}_{\mathrm{w}}$ and the feed forward gain factor $(\theta^*_{\hat{\mathrm{V}}_{\mathrm{w}}})'_{\hat{\mathrm{V}}_{\mathrm{w}}})$ are available, the feed forward control can be effectuated as proposed by eq.(4.6) and eq.(4.7) in subsection 4.1.3. Although for discrete use, first, this continuous expression should be converted by using a 'backward difference approach'

$$\dot{\theta}^*_{\hat{\mathrm{V}}_{\mathrm{w}}}[k] = (\theta^*_{\hat{\mathrm{V}}_{\mathrm{w}}})'_{\hat{\mathrm{V}}_{\mathrm{w}}}[k] \cdot \left(\frac{K_{\mathrm{D}}^{\hat{\mathrm{V}}_{\mathrm{w}}}}{T_{\mathrm{c}} + \tau_{\mathrm{D}}^{\hat{\mathrm{V}}_{\mathrm{w}}}} \cdot (\hat{V}_{\mathrm{w}}[k] - \hat{V}_{\mathrm{w}}[k-1]) \right) + \frac{\tau_{\mathrm{D}}^{\hat{\mathrm{V}}_{\mathrm{w}}}}{T_{\mathrm{c}} + \tau_{\mathrm{D}}^{\hat{\mathrm{V}}_{\mathrm{w}}}} \cdot \dot{\theta}^*_{\hat{\mathrm{V}}_{\mathrm{w}}}[k-1], \tag{4.18}$$

in which T_{c} is defined as the control cycle time. Finally, the conditional use of the feed forward contribution to pitch speed setpoint $\dot{\theta}^*$ can be implemented straightforward as described at the end of subsection 4.1.3.

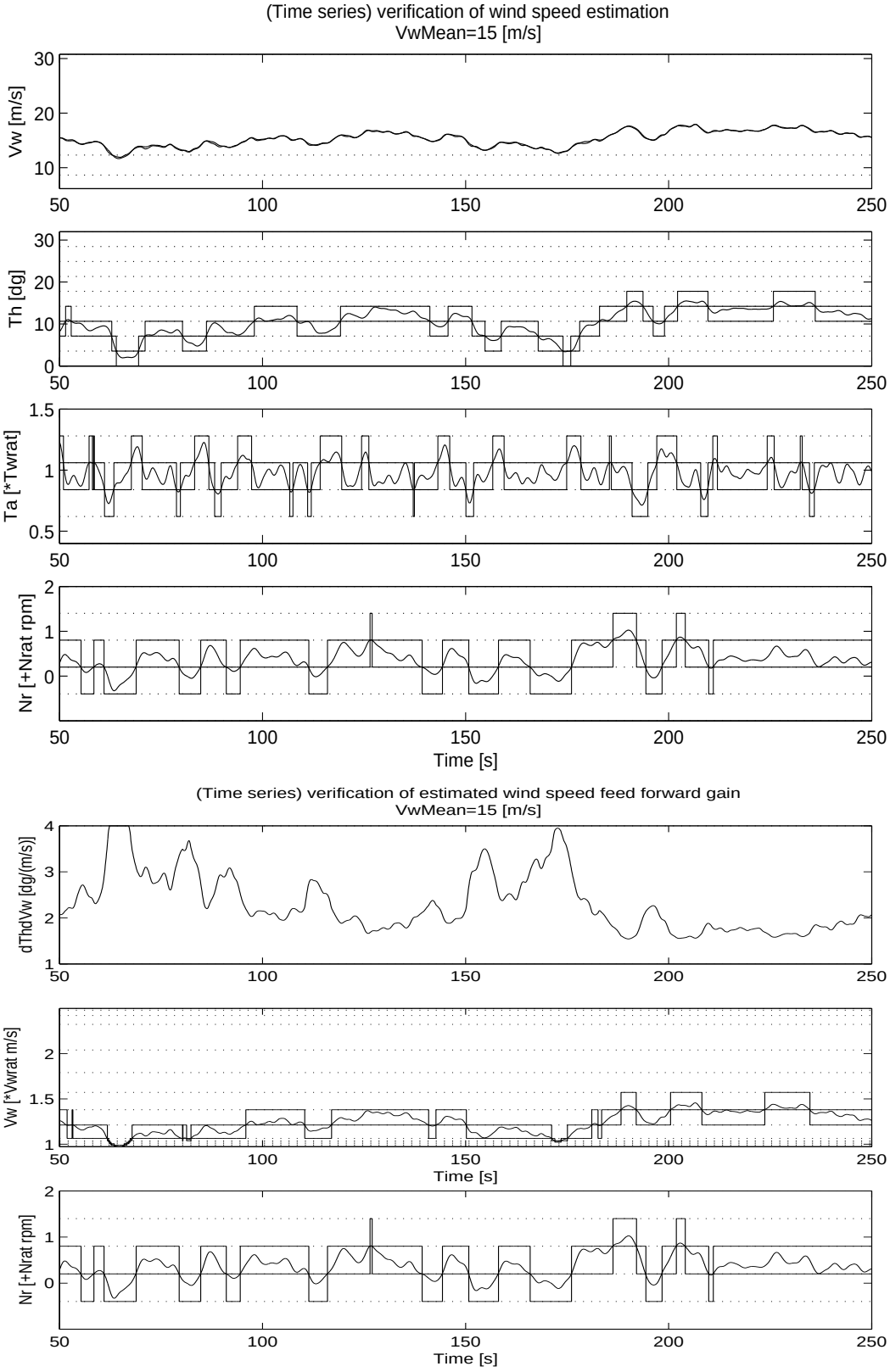

Figure 4.7: *Validation of estimated wind speed (upper 4 windows) and the feed forward gain factor (lower 3 windows) from previous simulation quantities; mean wind speed value above rated*

5 EVALUATION

In this chapter the control performance of 'feed forward of estimated wind speed' is verified by time domain simulations, stability analysis and parametric uncertainty behaviour.

5.1 Time domain simulation results

Time domain simulations were performed at two different mean wind speed levels (120% and 160% of rated wind speed), the control behaviour has been considered by comparing equal simulations with and without the feed forward structure.

All simulations were calculated for a typical megawatt sized turbine and with the power control structure as described in chapter 3 (including transition optimisation by electric torque actuation (see subsection 3.2.2): 0- 6% overtorque at pitch angle decrease from 10^o to 1^o). The rotor effective wind speed as described in section 2.4 was used; its time domain realisation for rated wind speed is shown in fig.(2.3). For the simulations the wind speed was scaled to 120% and 160% of its rated value by using eq.(2.10).

Although, the tabular implementation is preferable, the polynomial implementation of the feed forward of estimated wind speed was still used for the comparing simulations. The benefits of tabular implementation (section 4.2) are only of importance if the algorithm would be implemented in the turbine controller. For simulation results, there will be hardly any difference between both implementation approaches.

Each of the four simulations in the next sections show four windows, in which rotor speed, electric torque, electric power and pitch angle / pitch speed are respectively depicted. All quantities are normalised to their pertaining rated value.

5.1.1 Time domain simulation at 120% of rated wind speed

Fig.(5.1) shows time domain simulation results with and without feed forward at 120% of rated wind speed level. Taking a representative Weibull distribution into account (remote offshore at Nordsee) results in an increase of energy yield of 0.58% in this wind speed region. Due to the estimated wind speed feed forward the power production for this simulation is increased from 96.3 % to 97.9% . The standard deviation of the rotor speed (as a measure for fluctuation) decreases from 0.600 rpm to 0.446 rpm. The remaining power production dips are mainly due to (temporarily) below rated wind speed conditions, in all the situations the pitch angle is at (or nearly close to) the working position; this in contradiction to the simulation without feed forward.

Additionally, in fig.(5.2) both the estimated and (forced) uniform wind speed are shown. It is concluded that the estimated wind speed in the lower window is fairly similar to the uniform wind speed in the upper window.

5.1.2 Time domain simulation at 160% of rated wind speed

Fig.(5.3) shows time domain simulation results with and without feed forward at 160% of rated wind speed level.

Due to the estimated wind speed feed forward the power production for this simulation is increased from 97.9% to nearly 100%. Taking a representative Weibull distribution into account (remote offshore at Nordsee) results in an increase of energy yield of 0.24% in this wind speed region. The standard deviation of the rotor speed (as a measure for fluctuation) decreases from 0.718 rpm to 0.494 rpm. All power production dips are disappeared by improved pitch actuation, this in contradiction to the simulation without feed forward. Even the large wind gust around 600s is parried succesfully.

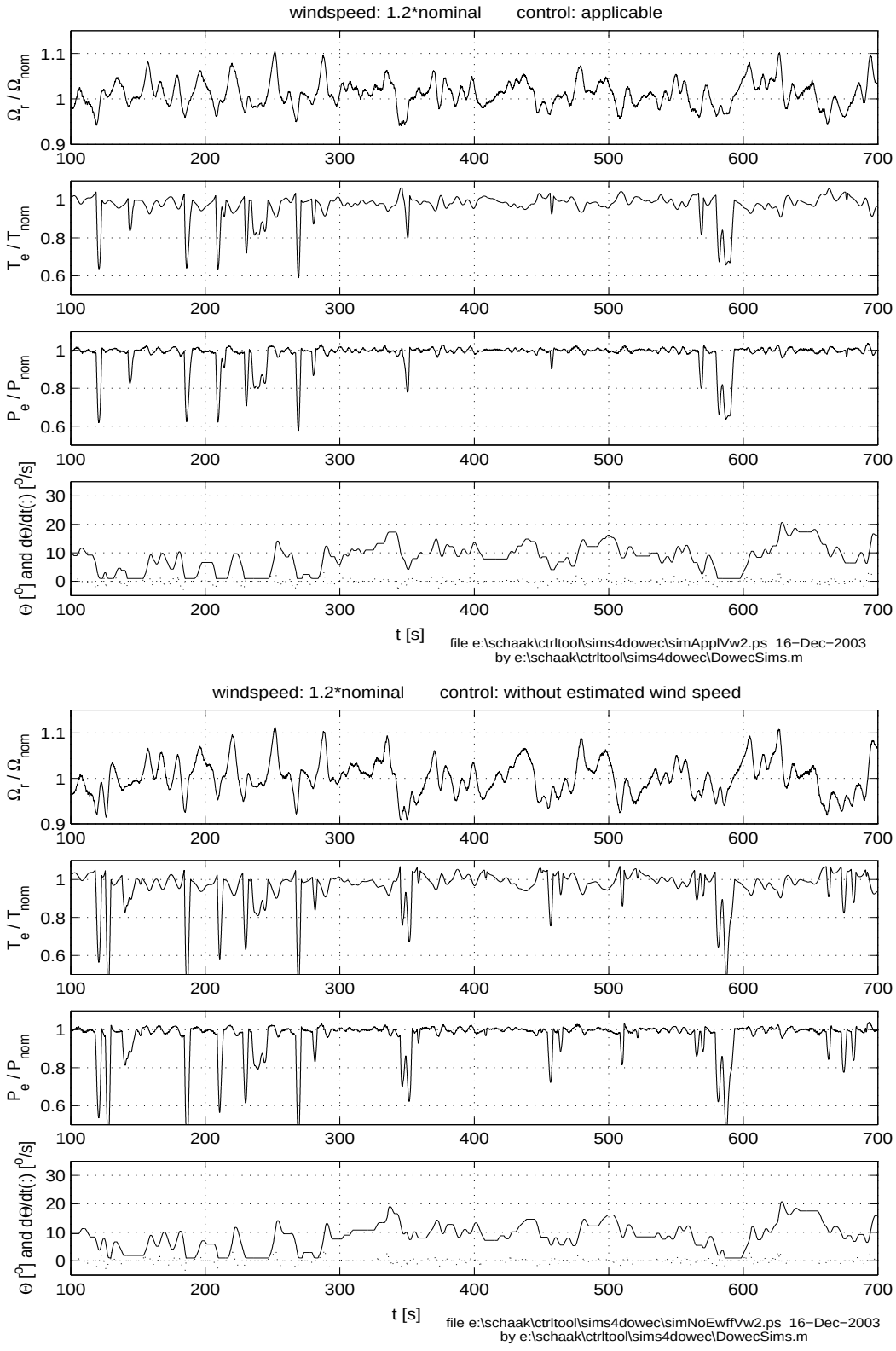

Figure 5.1: *Control performance at 120% of rated wind speed level; feed forward of estimated wind speed included (upper four windows) and excluded (lower four windows)*

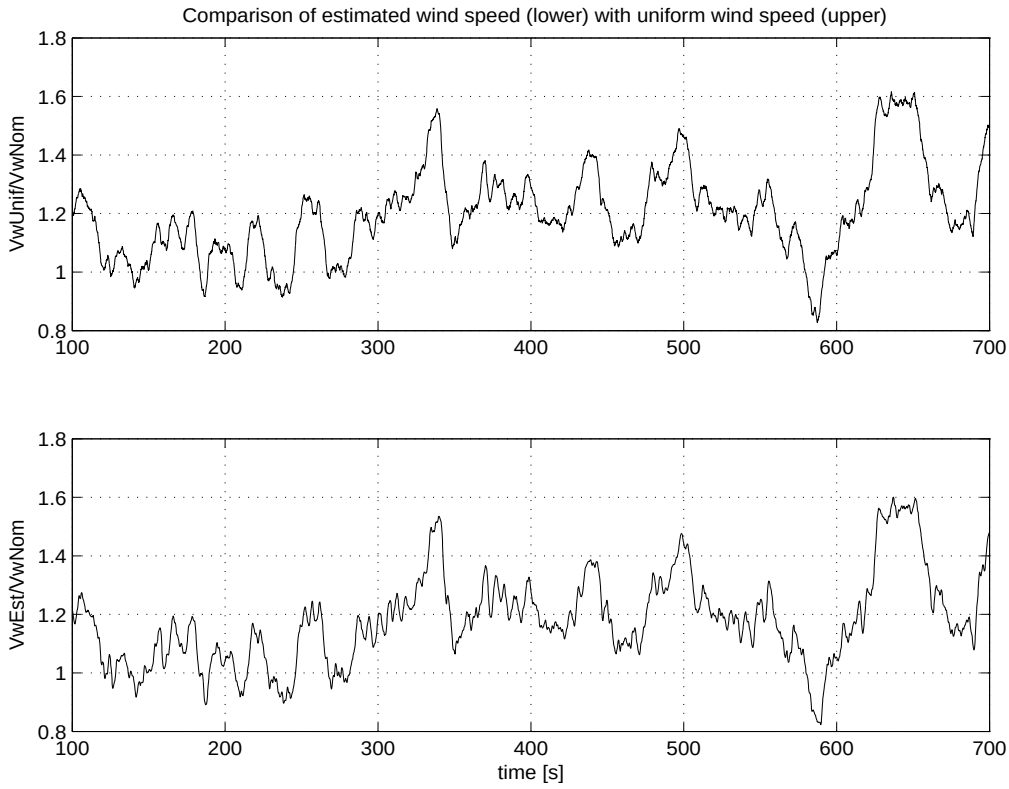

Figure 5.2: *Comparison of uniform wind speed (upper window) and estimated wind speed (lower window) at 120% of its rated level*

5.2 Frequency domain stability analysis

The PD controller full load pitch control structure as described in section 3.1.2 has been dimensioned in compliance with the stability law of Bode (gain margin 0.5 and phase margin 45^o). This was performed at the operation point at which maximum torque to pitch angle sensitivity occurs. Nyquist diagrams for each relevant operation point were calculated to check the stability in the whole operation area of the wind turbine. The (open loop) rotor speed transfer function for stability analysis incorporates all relevant modelling aspects in linearised format over the whole operation envelope (see also [3])

1. stiff drive train dynamics;
2. aerodynamic torque to pitch angle sensitivity (process gain);
3. scheduled PD-compensator;
4. rotor speed cascade filter;
5. second order pitch actuator dynamics;
6. electric torque influence by generator through speed/torque curve;
7. direct aerodynamic torque influcence by rotor speed;
8. indirect aerodynmaic torque influence by pitch angle and rotor speed through fore/aft tower movement;

The effect of the estimated wind speed feed forward is examined by comparison of Nyquist analysis without and with the feed forward structure (fig.(5.4)).

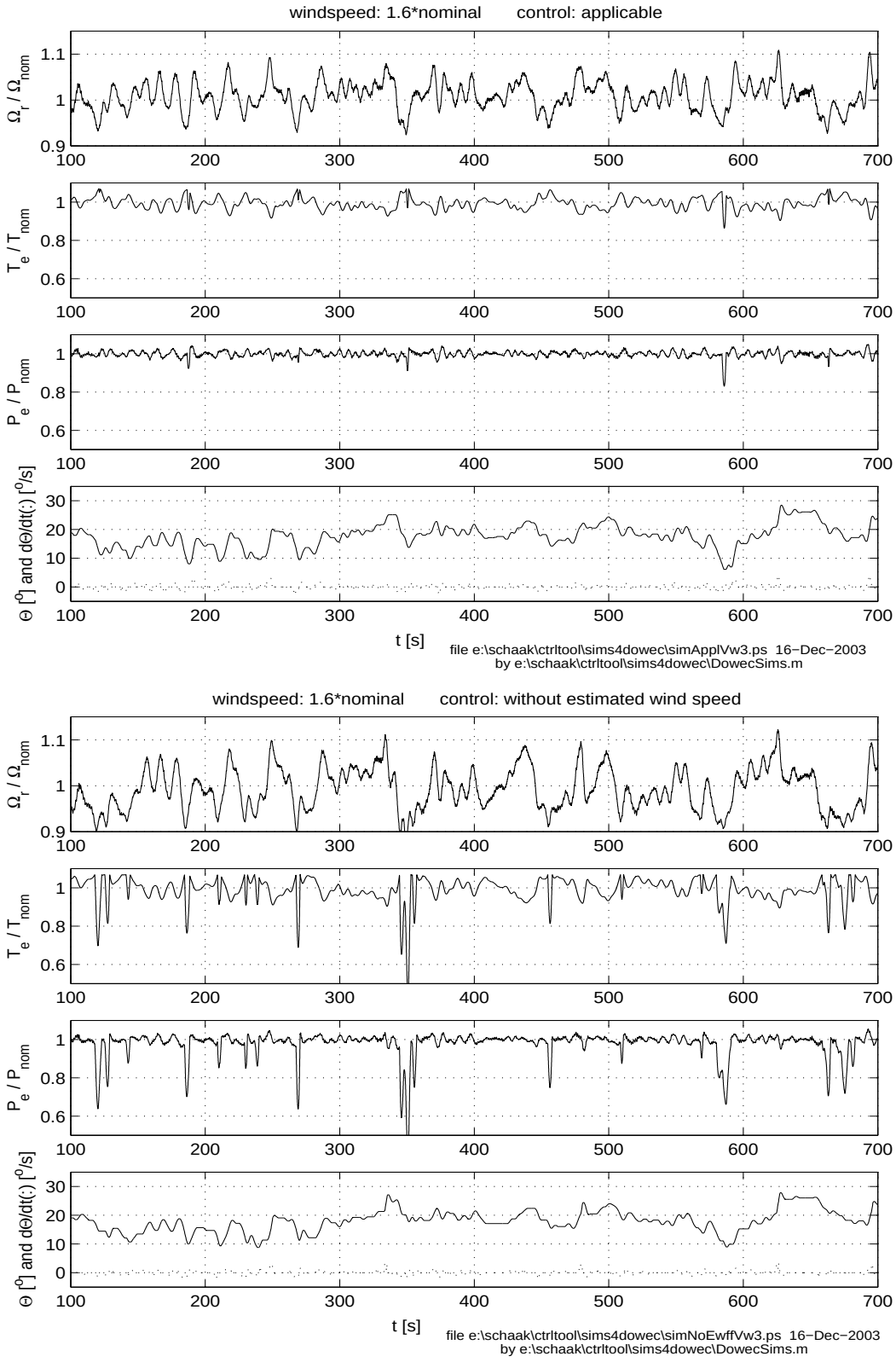

Figure 5.3: *Control performance at 160% of rated wind speed level; feed forward of estimated wind speed included (upper four windows) and excluded (lower four windows)*

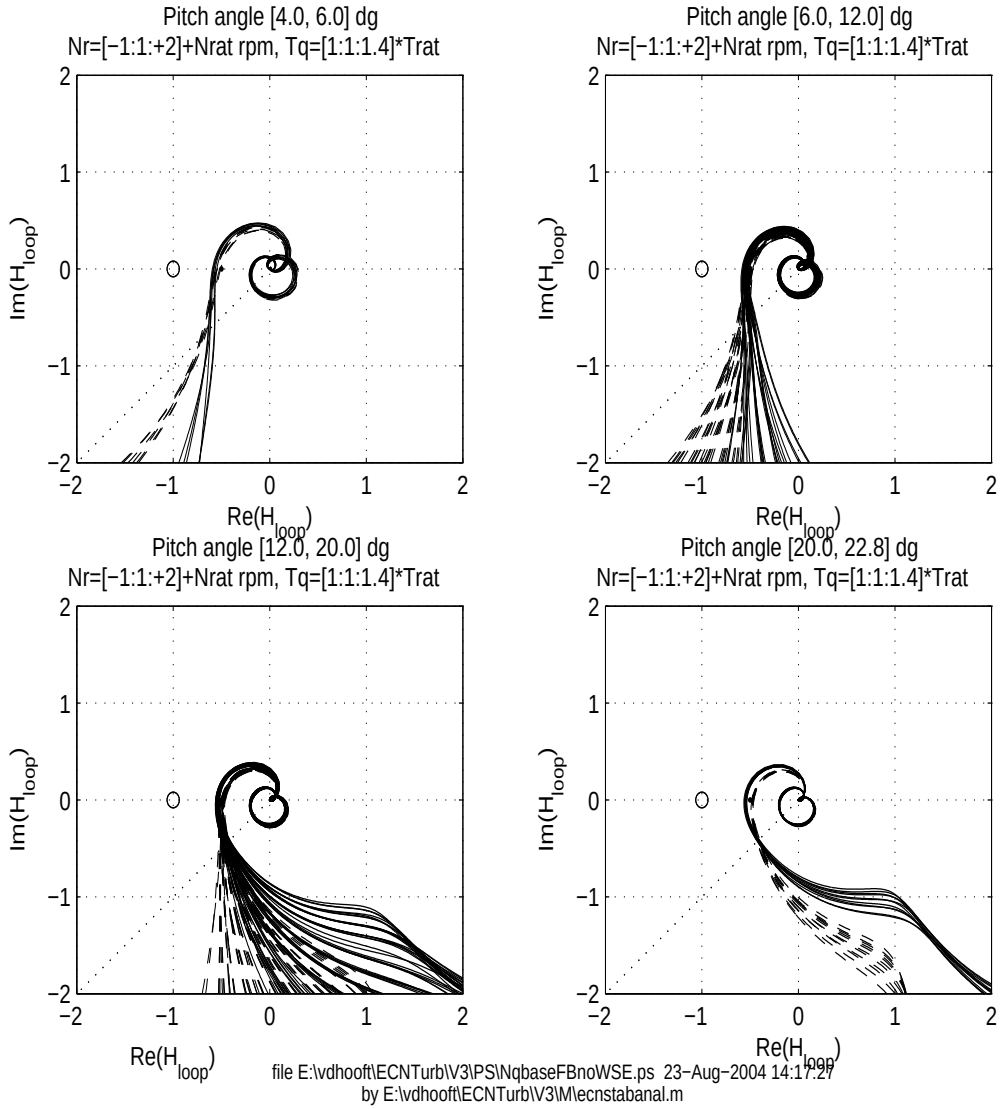

Figure 5.4: *Stability diagrams without (dashed) and with the feed forward structure (solid)*

All Nyquist contours are passing the (-1,0) point with increasing frequency at the right side, which implies stability of the closed loop system. Additionally, the design amplitude margins (0.5) and phase margins (45 $^{\circ}$) are hardly affected after incorporation of the feed forward structure (solid lines). Even, it can be concluded that the feed forward structure improves the robustness and stability behaviour because the tails of the Nyquist contours are counterclockwise shifted: this is due to the phase lead effect of DD-control (subsection 4.1.3).

5.3 Parametric uncertainty behaviour

As discussed in section 4.1 the estimation of uniform wind speed is also dependent of a priori knowledge of the aerodynamic torque coefficients $\hat{C}_{\rm q}(\tilde{\theta}^{\rm f},\hat{\lambda})$, the rotor radius $\hat{R}_{\rm b}$ and the air density $\hat{\rho}_{\rm air}$and the total inertia $\hat{J}_{\rm t}$In practice these values will differ from the values as assumed during design. To check the behaviour for these practical parameter uncertainties, additional simulations were done with deviated parameters (over- and under estimated values) for the whole wind range. Both the relative error and of the estimated wind speed value and the relative difference of estimated wind speed variations were observed.

The following conclusions were made:

- torque coefficients are most uncertain during design; bad estimation of the torque coefficients during design with +/-20% results in a relative error of about -/+10% in the estimated wind speed around rated wind speed conditions, while it decreases to -/+4% at cut-out condition; there's hardly any difference in wind speed variations;
- accurate estimation of the rotor radius is easy, feasible deviations during design of +/-1% results in a relative error below -/+1%, while difference in wind speed variations occurs specific around rated conditions ($\sim$2%);
- air density can vary in time and will be site dependent, mismatch during design with +/-5% results in a relative error of about -4% and +1.5% respectively in the estimated wind speed around rated wind speed conditions, while it decreases to -/+1% at cut-out condition; difference in wind speed variations occurs specific around rated conditions ($\sim$2%);
- total rotor inertia can be calculated accurately; it is of no importance for the estimated wind speed value, but it causes undesired variations in the estimated wind speed; although a mismatch of 10% has hardly any effect.

It can be concluded that parameter deviations results in an offset of the estimated wind speed, although there were no extreme sensitivities found within the range of practical deviations of the involved parameters. Because the derivative of the wind speed is used for effectuation in the control loop these offsets are of no importance. Increase of variations can be a problem, however this is not expected because the rotor radius en rotor inertia are accurate to determine. Additionally, a low pass filter will smooth these fluctuations before actuation.

Fig.(5.5) shows a typical worst case situation of combined deviations ($\hat{C}_{\mathrm{q}}(\tilde{\theta}^{\mathrm{f}},\hat{\lambda})$ =-15%, $\hat{R}_{\mathrm{b}}$ =-1% $\hat{\rho}_{\mathrm{air}}$ = -5% and $\hat{J}_{\mathrm{t}}$ = +10%.) In this figure the o-dotted lines are with parameter deviations included and the solid lines are representing the relative error in the estimated wind speed. It results in a relative error of about +12% in the estimated wind speed around rated wind speed conditions, while it decreases to +5% at cut-out condition. Cumulation of errors takes hardly place.

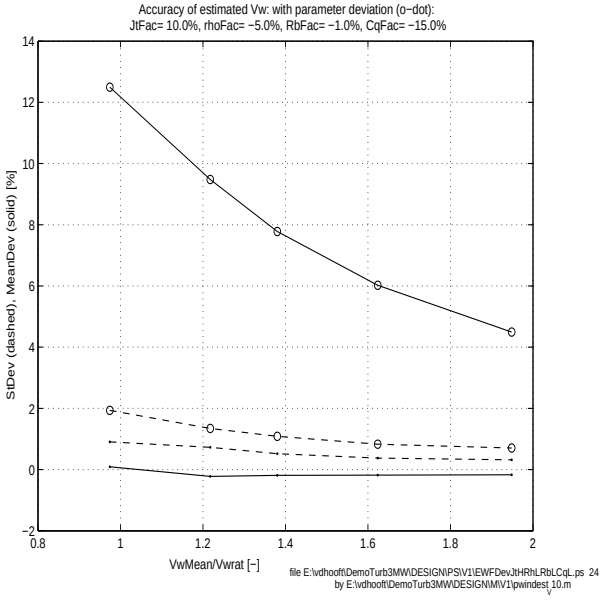

Figure 5.5: *Worst case situation of combined parameter deviations; with (o-dotted) and without (.-dotted) deviations; relative error in wind speed value (solid) and relative difference in variations (dashed)*

6 CONCLUSIONS

Inclusion of a feed forward of estimated wind speed control action, has shown to be a powerful extension to current ECN wind turbine control structures.

In time domain simulations, inclusion of a feed forward of estimated wind speed control action has shown to be a powerful extension to current ECN wind turbine control structures:

- reduction of rotor speed variations: ~ 0.2 rpm decreased standard deviation;
- improved turbine behaviour to large wind gusts;
- increase of energy yield of $\sim 0.9\%$;

For reasons of simplicity and robustness, a tabular implementation approach is preferred above polynomial implementation.

Prior solving of the complicated implicit relations for the estimated wind speed and the feed forward gain factor and storing the solutions in data tables for on-line use during algorithm execution, have been resulted in a brief, effective, control algorithm.

Definition of an appropriate operation area and design of a quick search and interpolation algorithm has resulted in small sized tables and low hardware requirements.

A minimum number of easy interpretable parameters is required for design of tables and tuning of the algorithm.

Both stability, robustness and parametric uncertainties were observed. The addition control loop has a slightly positive effect on overall stability and robustness. Appeared offsets in the estimated wind speed value due to parameter uncertainties do not have impact on the effectuation of the wind speed feed forward loop.

REFERENCES

[1] Int. Electrotechnical Commission. Wind turbine generator systems - part 1: Safety requirements. Technical Report IEC 61400-1, IEC, February 1999.

[2] T.G. van Engelen, E.L. van der Hooft, and P. Schaak. Ontwerpgereedschappen voor de regeling van windturbines. Technical Report ECN-I–00-xxx, ECN Petten, In preparation to issue 2004.

[3] E.L. van der Hooft, P. Schaak, and T.G. van Engelen. Wind turbine control algorithms; DOWEC-F1W1-EH-03-094/0. Technical Report ECN-C–03-111, ECN Petten, December 2003.

[4] P. Schaak. Koppelregeling van variabel-toeren windturbines. Technical Report ECN-C–03-136, ECN Petten, December 2003.

	Date: December 2003	**Report No.:** ECN-C–03-137
Title	Feed forward control of estimated wind speed	
Author	E.L. van der Hooft; T.G. van Engelen	
Principal(s)	Novem	
ECN project number	7.4153	
Principal's order number	2020-01-12-10-003	
Programmes	BSE DEN 2001	

Abstract

A control structure 'feed forward of estimated wind speed' is described, as it were: 'the wind turbine rotor will be used as a wind meter'.

The control structure is based on 'estimation' of wind speed as well as a non-linear compensation of a wind speed dependent pitch speed setpoint, which is optimised to maintain (stationary) rated electric power. It is required to know the rotor properties with moderate accuracy.

In time domain simulations, inclusion of a feed forward of estimated wind speed control action has shown to be a powerful extension to current ECN wind turbine control structures:

- reduction of rotor speed variations: $\sim$ 0.2 rpm decreased standard deviation;
- improved turbine response to large wind gusts;
- increase of energy yield of $\sim$ 0.9%;

For reasons of simplicity and robustness, a tabular implementation approach is preferred above polynomial implementation. The resulting brief algorithm uses small sized tables, requires low hardware requirements and needs a minimum of easy interpretable parameters for design and tuning.

Both stability, robustness and parametric uncertainties were observed. The addition control loop has a slightly positive effect on overall stability and robustness. Appeared offsets in the estimated wind speed value due to parameter uncertainties do not have impact on the effectuation of the wind speed feed forward loop.

Keywords

Wind turbine control, Pitch Control, Power Control, Optimisation, Variable speed control

Authorization	**Name**	**Signature**	**Date**
Checked	P. Schaak		
Approved	H.B. Hendriks		
Authorised	H.J.M Beurskens		